Journal of Materials Chemistry A

Accepted Manuscript

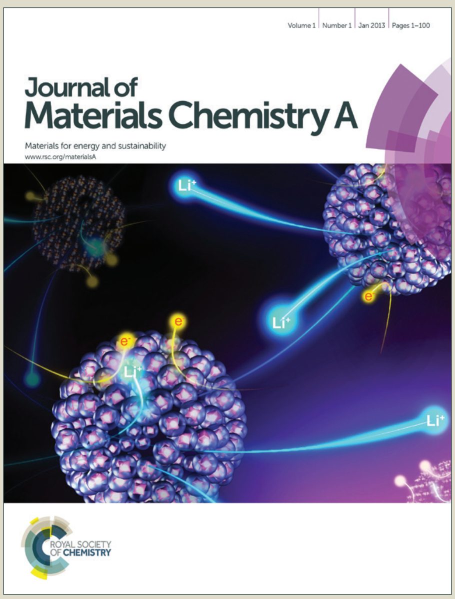

Flexible Fiber/Wire Shaped Solar Cells in Progress: Properties, Materials, and Designs

Ming Peng[a] and Dechun Zou[a, b, c*]

[*] Prof. Dechun Zou (E-mail: dczou@pku.edu.cn)

[a]Beijing National Laboratory for Molecular Sciences, Key Laboratory of Polymer Chemistry and Physics of Ministry of Education, College of Chemistry and Molecular Engineering, Peking University, Beijing 100871, China. Tel/Fax: +86-10-6275-9799.

[b]Beijing Research Center of Active Matrix Display Technology, Peking University, Beijing 100871, China.

[c]Beijing Institute of Nanoenergy and Nanosystems, Chinese Academy of Science, Beijing 100083, China.

Abstract

Flexible fiber/wire-shaped solar cells are kind of photovoltaic cells fabricated on wire-like substrates. Fiber-type devices, including inorganic, organic, dye-sensitized and perovskite solar cells, have made great progress in the recent years. Especially, the energy conversion efficiency of fiber dye-sensitized solar cells has increased from < 0.5% to > 9%. In this review, we provided very detailed insights into the development of various fiber/wire-shaped solar cells, conventional materials, and innovative designs. Particularly, we focused on the properties of fiber dye-sensitized solar cells, the innovations for solar energy harvesting, and the integrated power

systems for electrochemical energy conversion and storage. Although recent studies only provided the initial ideas, flexible fiber/wire-shaped solar cells facilitated the breakthrough for novel solar architecture and portable/wearable electronics or e-textiles of the future.

Keywords: fiber/wire shaped solar cells; integrated power systems; energy conversion and storage; portable/wearable electronics

Introduction

Energy and environmental issues are two of the most prominent problems in modern society. For sustainable development, scalable and clean energy conversion via solar cells has attracted both academic and industrial attention since the foundation of photoelectric effect. The past years have witnessed the expanding market of photovoltaic cells based on Si, CdTe and CIGS ($Cu(In,Ga)(S,Se)_2$), as well as the rapid development of new photovoltaic generations, such as CZTS ($Cu_2ZnSn(SSe)_4$), organic solar cells, dye-sensitized solar cells (DSSCs), and perovskite solar cells[1, 2]. In particular, the report by National Renewable Energy Laboratory indicated that the solar cell types and optimal research-cell efficiencies have been continuously refreshed in the past 40 years[3]. The most significant feature of typical solar cells is the planar shape with dimensional extension. Thus, the development of one- or three-dimensional (1D or 3D) photovoltaic cells will break through the limitations of conventional thinking and generate a new concept for solar energy conversion. This vision could also create opportunities for material science/structure design that would be interesting as technical innovations and beneficial for special energy applications.

With the rapid development of traditional industry and increasing demand of modern electronics, the integrated optoelectronic products come to the age of small, portable, lightweight and smart merchandise. In recent years, wearable/portable electronics, such as Google glasses, iWatch, and smart phone, have gradually become part of human lives. To deepen the wearable concept and meet future individual needs, incorporating flexible optoelectronic devices (e.g., sensors, logic circuits, antenna, lighting elements, and power systems) in clothing, backpacks, and other belongings would become an important trend for the next generation of smart products, namely "electronic textiles" or "e-textiles"[4, 5]. The fundamental functional units for e-textiles remain to be developed. Especially, flexible power sources with efficient energy conversion and storage can automatically generate electricity and contribute to self-driven energy systems[6-8], which are very promising candidates for the portable/wearable electronics that can further enrich e-textiles[9-11]. Among the energy technology innovations, flexible fiber/wire-shaped energy devices, including solar cells, batteries, supercapacitors, light-emitting diodes, and field-effect transistors, are booming in recent years and attracting increasing attention[12-18]. Flexible fiber/wire-shaped energy devices fabricated on fiber- or wire-type conductive substrates are the suitable units for contexture because of their special linear shape and may play a role in practical e-textiles, such as wearable solar power sources and self-powered smart systems. In particular, fiber/wire-shaped solar cells demonstrate solar-to-electric conversion but comprise special photovoltaic architecture fabricated on fiber substrates, which endow the devices special properties and allow innovations.

Since 2010, several reviews have scanned the basic principle and conventional device structures of fiber-like solar cells[12-14]. However, the coverage and concept have been spreading because of the rapid expansion of this emerging research field in the last three years. For clarify the development tendency, the development of flexible fiber/wire-shaped solar cells, including inorganic, organic, dye-sensitized, and perovskite photovoltaic fibers, are presented. Focus was given on the properties, materials, and designs of fiber-shaped dye-sensitized solar cells (FDSCs) because they are the most developed type and could provide certain guidance to the other types. The shortcomings of recent research and future development were also summarized on the basis of status quo. In the present review, a very detailed insight into the development of fiber solar cells was provided in Part 1, covering research motivation, conventional materials, structure designs, and future perspectives. Properties of fiber solar cells associated with structure design were discussed in Part 2. Attention was paid to the materials explorations of FDSCs in Part 3; and solar devices with special energy harvesting design were provided in Part 4 to broaden the fiber based innovations. In Part 5, the cases that fiber solar cells integrated into hybrid systems were highlighted for energy management. Given the rapid development, works until March 2015 were summarized, and a fast development momentum for this highly growing field may exist in the future.

1 Development of Fiber-Shaped Solar Cells

The preliminary concepts of fiber/wire shaped solar cells appeared in some patents since the 1980s, in which silicon layers formed p-n or p-i-n junctions on conducting fiber substrates to obtain a low-cost and flexible devices[19]. The real progress of this field started at the beginning of 21st century, where new types of fiber solar cells and structure designs are booming up with rapid development of photovoltaic field[13, 19-28]. The past records of fiber solar cells is presented in **Figure 1**; and continuing development context of fiber inorganic, organic, dye-sensitized, perovskite solar cells is summarized from Part 1.1 to 1.4, respectively.

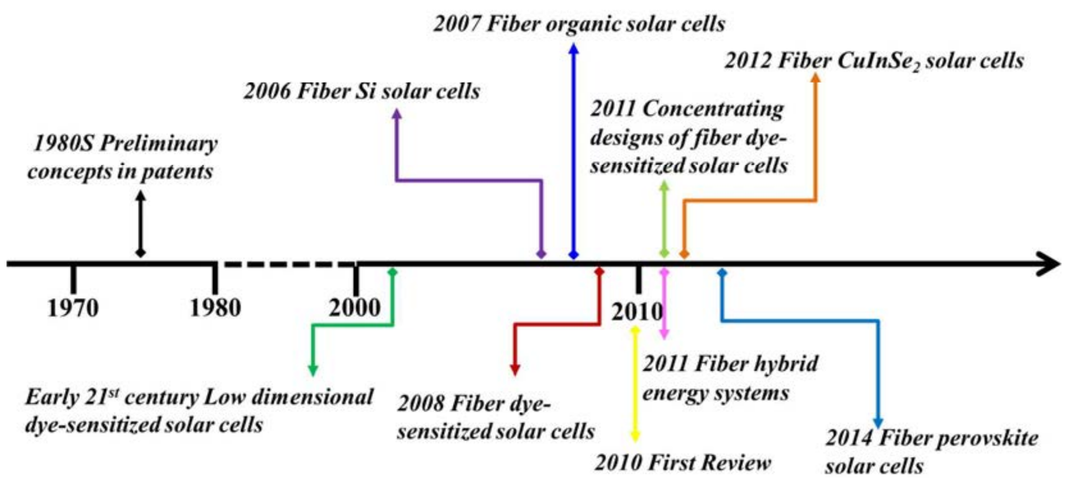

Figure 1 Past records of fiber solar cells[13, 19-28].

1.1 Fiber Inorganic Solar Cells

Silicon solar cells, based on the high natural abundance element, have experienced a long research history. The excellent reliability and acceptable cost make them mainstream products in the photovoltaic market. Silicon technology based on vapor deposition could be adapted to different substrates, and it is a good choice to construct solar cells and detectors on flexible fibers. Early explorations since 2006 have claimed flexible fiber-type poly-Si solar cells on glass fiber[22] and carbon fiber[29], but the device performance were very low. In 2013, Badding et al[30] fabricated flexible coaxial silicon fiber pores with p-i-n photodiode junction (**Figure 2**) through high-pressure chemical vapor deposition. Flexible silicon fibers with length of up to 10 m were deposed, which demonstrated a potential for scalable preparations. The low light absorption of the active layers resulted in an overall conversion efficiency of 0.5%. Later on, Gibson et al.[31] reported silica sheath fibers by using bulk glass draw techniques with low purity p-type silicon polycrystalline as starting material. The silica that formed into silicon core was etched from one side and deposed with a-i-Si and a-n-Si layers via PECVD to form a p-i-n junction. The silicon-core glass fiber achieved efficiencies of up to 3.6%, leaving room for improvements over the presented prototype. Except Si fibers, Chen et al.[27] prepared flexible fiber-shaped $CuInSe_2$ (CIS) solar cells by ordinal electro-deposition of $CuInSe_2$ layer, chemical bath deposition (CBD) of CdS, and then RF magnetron sputtering of ZnO and ITO layers on the Mo wire (**Figure 3a**). The single-wire solar cell achieved energy conversion efficiency of up to 2.3% and exhibited excellent long-time stability (stored at 60 ^{o}C for 0-600 h) (**Figure 3b**).

Mature preparation based on silicon industry, scalable technology via vapor deposition, and reliable stability of all-solid devices are the advantages of inorganic fiber solar cells, which are the key points for wearable electronics. However, a long period of efficiency improvement occurred, which remains an important issue in future development. Significant improvement and great chances for applications are available considering the performance of traditional inorganic photovoltaic cells and the solid foundations of silicon industry.

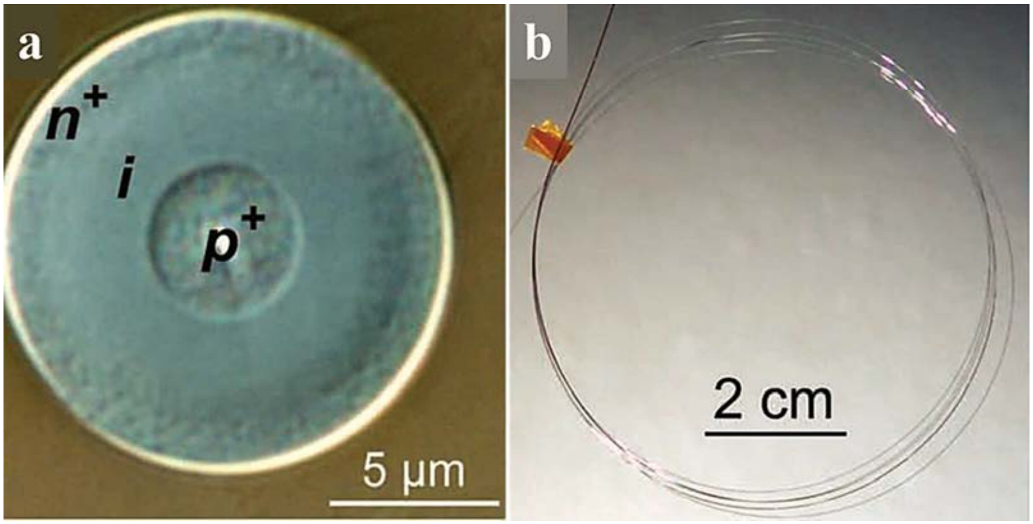

Figure 2 (a) Differential interference contrast optical micrograph of a representative 15 μm diameter Si p-i-n junction; (b) Flexible silicon fiber solar cell of ~1 m long based on p-i-n junction[30]. Reproduced from Ref. 30 with permission, Copyright © 2013 WILEY-VCH Verlag GmbH & Co. KGaA, Weinheim.

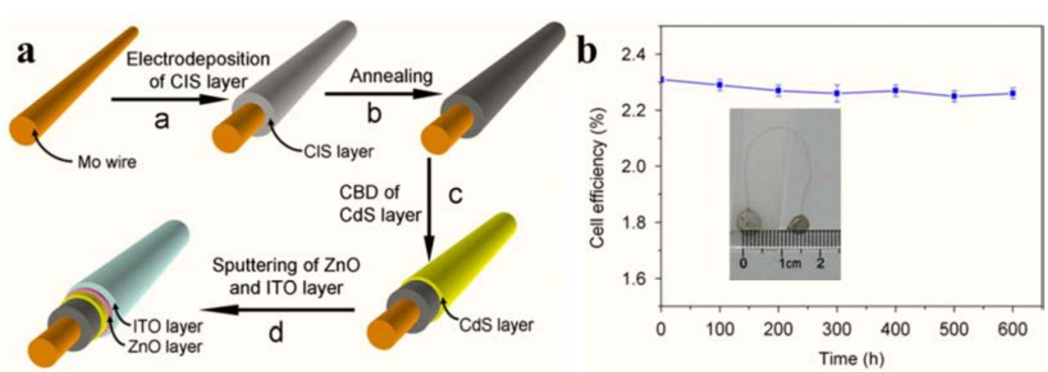

Figure 3 (a) Fabrication of Mo/CIS/CdS/ZnO/ITO single-wire flexible solar cells; (b) The time-dependent change in the conversion efficiency of the single-wire solar cell

stored at 60 ^{o}C for 0-600 h. Inert is the photo of single-wire device[27]. Reproduced from Ref. 27 with permission, Copyright © 2012 Elsevier Ltd.

1.2 Fiber Organic Solar Cells

In traditional planar organic photovoltaics, efficient charge transport and optimal optical absorption was usually not capable. To break through this contradiction, Carroll and co-workers[23, 32] demonstrated fiber organic solar cells based on waveguide optical geometries in 2007 (**Figure 4**). The device with a structure of optical fiber/ITO/PEDOT:PSS/P3HT:PCBM/LiF/Al achieved efficiency of 1.1%[32, 33]. But the optical fibers are relatively expensive and less flexible for weaving cases. Flexible polyimide-coated silica fibers and polypropylene fibers were demonstrated as possible alternative substrates for organic photovoltaic fibers via evaporation or solution process[34, 35]. Driven by the goal of efficient light absorption in wide incident angles and more freedom of physical appearance, non-planar cylindrical devices with tube and glass rod substrate were also created, with efficiencies from 0.6% to 1.4%[36, 37]. Equivalent circuit model analysis found that the aspect ratios to obtain the optimum overall optical confinement and optimal power conversion performance were between 1 and 5[38]. To eliminate usage of transparent oxide semiconductors, Gaudiana et al.[39] reported efficient flexible organic photovoltaic fibers with efficiency of up to 3.9% in 2009. In their design, two twisted functional fibers, one comprising a conducting polymer and fullerene derivative and the other coated with a silver film, were wrapped together and encased. In further attempts to replacing the metal counter electrode, a carbon nanotube (CNT) fiber was used to twist the fiber anode with TiO_2/P3HT:PCBM/PEDOT:PSS layers, and the photovoltaic wires achieved efficiency of up to 1.8%, which maintained by ~85% after bending (bending radii of ~5 mm) for 1000 cycles[40, 41]. Cao and co-works[42, 43] demonstrated that CNT films, CNT yarns (**Figure 5a** and **5b**), and single-layer graphene as counter electrodes can contribute to 2.3% to 2.5% efficiency. The devices show stable behavior during bending and moderate stability under inertia gas for 20 days (**Figure 5c** and **5d**). Especially, involving carbon based film as the second electrode could avoid thin layers penetrating during twisting, maintain good interface contact to the inner layer and provide satisfying light transparency. In further attempts, flexible, lightweight, easy-processable organic photovoltaic textiles (**Figure 6**) with reasonable photovoltaic performance were developed, which provide a promising avenue toward wearable electronics[44, 45]. Light harvesting, oscillator strength, and low charge mobility limitations are the hindrances toward efficient organic solar fibers, but cost-competitive and large-scale fabrication of traditional organic solar platforms are claimed to be possible[46]. Moreover，17% efficiency can be achieved using theoretical calculations in a reflective tandem architecture[47].

Organic photovoltaics provide material basis for flexible and stable fiber solar cells, which simulates wide research motivation for wearable solar power sources. Though solution process would bring much convenient in film preparation, dip-coating rather than conventional spin-coating is used to deposit the active layers for fiber/wire type organic solar cells. The difficulties in preparing long-range, uniform, and controllable thin films and forming efficient interface junctions on curved surface is a real technical challenge for highly efficient organic fiber devices. Further research would see the corporation of novel organic/polymer photovoltaic materials, improved functional interfaces and advanced optical structures.

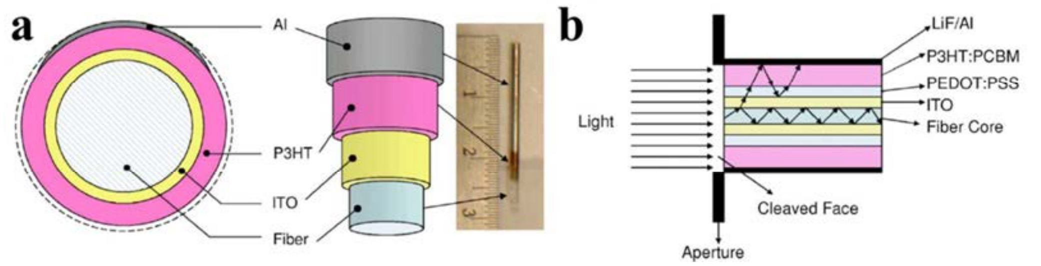

Figure 4 Organic fiber solar cell based on optical fiber (a) and its light harvesting path (b)[32]. Reproduced from Ref. 32 with permission, rights managed by AIP Publishing LLC (2007).

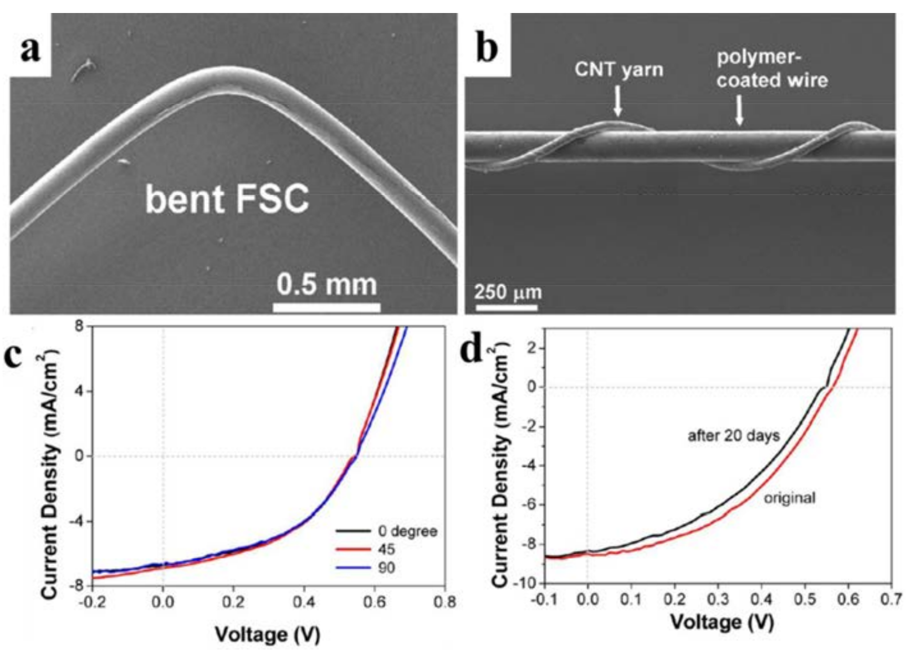

Figure 5 (a) Organic fiber solar cell with CNT films as counter electrode (bent to nearly 90 degrees). (b) Organic fiber solar cell based on CNT yarns. (c) *J*-*V* curves of

a CNT films based organic fiber solar cell in straight form (0 degree) and bent to 45 and 90 degrees, respectively, showing stable behavior during bending. (d) *J-V* curves of the CNT yarns based organic fiber solar cell in original state and after storage in inertia gas for 20 days[42]. Reproduced from Ref. 42 with permission, Copyright © 2012, American Chemical Society.

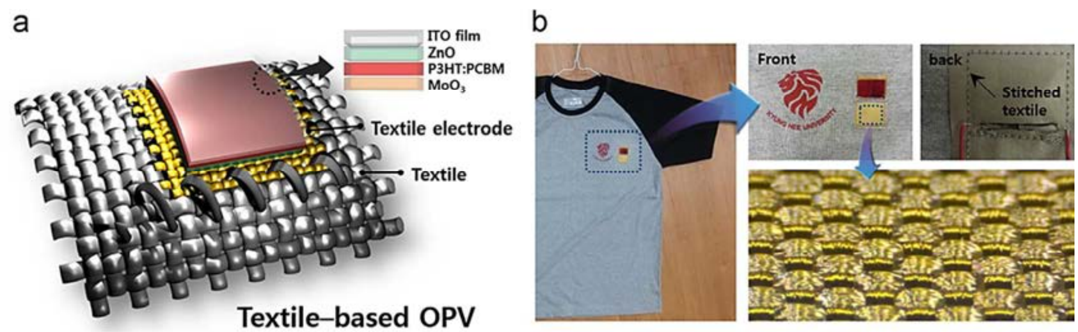

Figure 6 (a) Concept of a stitchable organic photovoltaic textile. (b) Photographs of the textile-based OPV integrated with clothing[45]. Reproduced from Ref. 45 with permission, Copyright © 2014 Elsevier Ltd.

1.3 Fiber Dye-Sensitized Solar Cells (FDSCs)

The tentative idea of FDSCs took shape at the beginning of the 21st century, which made advantages of the simple, air-tolerant, and robust DSSC preparation[48] and extended the typical sandwich device to lower dimensional structure[20, 21]. In 2008, Zou et al. reported flexible wire-like DSSCs based on double twisted metal fibers (**Figure 7a**)[24]. This design featured as linear shape, transparent conductive oxide (TCO)-free and easy fabrication attracted wide attention[49]. Later on, singly twisted FDSCs where the counter electrode (Pt wire) winding the fiber photoanode (**Figure**

7b) were prepared and the device with capillary package achieved efficiency up to 7%[25, 50]. The above success led to follow-up FDSC explorations toward higher efficiency, cheaper materials, larger device size, better stability, concentrated designs and energy management, which included: 1) selection of commercial, inexpensive, lightweight fiber substrates for improved surface area and light harvesting; 2) synthesis of nano materials and interface engineering for efficient fiber photoanodes; 3) development of cost-effective and highly active catalyst for counter electrodes; 4) low volatile electrolyte for improved device stability; 5) novel designs of fiber electrodes for 3D solar cells and concentrated devices; 6) integrated fiber energy system for multi-step energy conversion and storage.

All the trials and errors contributed to the continuous FDSC performance improvement, from < 0.5% to > 9% throughout the years[51, 52]. For example, well-designed device conformation, film preparation and interface engineering on fiber photoanodes improved dye-adsorption amount, enhanced light collection, better electron injection, and inhibited charge recombination, thereby achieving 7.2% to 8.6% efficiency[53-55]. Ultra-long FDSCs of more than 30 cm were fabricated with efficiency up to 4% (aspect ratio of 310), which are the longest single FDSCs with the highest power output and could be applied to solar fabrics (**Figure 7c** and **7d**)[56, 57]. For price considerations, replacing Pt-based counter electrode with cost-effective materials with high specific area is a sustainable way, achieving efficiencies of 7.2% to 8.5%[58, 59]. To take a further step toward lightweight and inexpensive power sources, non-metal wire substrates have been applied to either or both electrodes[60-63]. Especially, all-carbon based FDSCs[60] and quantum dot (QDs) sensitized fiber solar cells[64] with moderate device performance were developed, and more breakthroughs are on the way. Typical volatile liquid electrolyte may prevent device stability in the long run, whereas gel and solid electrolytes can reasonably supply the solutions for stable FDSCs[65-67]. FDSC exploration was also expanded to innovations concerning light collection for high power output. Given the symmetric columnar structure, fiber photoanodes endowed FDSCs with capacities such as 3D light harvesting and less-independent incident light angles, which contributed to flexible multi-fiber solar device of 9.1% efficiency[52] and concentrating modules with fold-improved power output[25, 68]. Except for solar-to-electrical generation, highly performing FDSCs can be integrated with other fiber shaped energy conversion devices, such as supercapacitor, battery and nanogenerator, for hybrid energy systems[26, 69, 70], thereby providing more flexible energy management.

From the view of energy conversion efficiency, the performance of FDSCs is very close to traditional planar DSSCs. The development of FDSCs could represent the directions of all fiber solar cells, namely, 1) new materials and interface engineering for continuously improved performance; 2) efficient fiber electrodes for structure designs; 3) advanced solar energy system based on fiber photovoltaics. All the attempts and progress will push the fiber photovoltaics to higher level, and make chance for practical solar power for portable/wearable electronics.

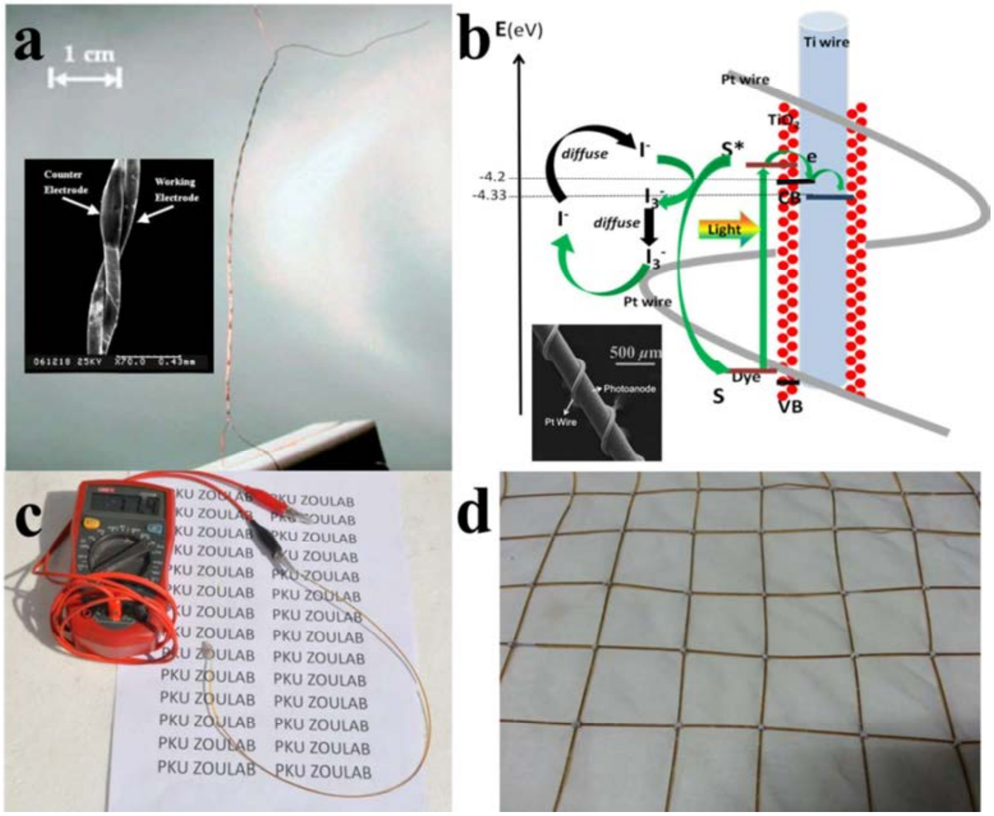

Figure 7 (a) Flexible wire-like dye-sensitized solar cell based on twisted metal electrodes[24]. Reproduced with permission from ref. 24, Copyright © 2008 WILEY-VCH Verlag GmbH & Co. KGaA, Weinheim. (b) Schematic of singly twisted FDSCs where the counter electrode (Pt wire) winding the fiber photoanode with working mechanism[25]. Reproduced from Ref. 25 with permission from the Royal Society of Chemistry. (c) Ultra-long FDSC of more than 30 cm (with aspect ratio of 310) displays *I*sc of 11.4mA under natural light conditions (13:50 on October 16, 2013); (d) Flexible fabric of flexible FDSCs on the cloth substrate[56]. Reproduced from Ref. 56 with permission from the Royal Society of Chemistry.

1.4 Fiber Perovskite Solar Cells

The new photovoltaic generation, perovskite solar cells[71] have attracted worldwide attention, whose efficiency has been improved to > 20% in five years[3]. Solid state, high performance and easy solution processing are the notable features of perovskite solar cells, which make them suitable candidates for efficient, flexible, lightweight, and liquid-free photovoltaic fibers. Peng's group[28] demonstrated perovskite fiber solar cells (**Figure 8**) by winding an aligned multi-walled carbon nanotube sheet onto a TiO_2-modified steel wire (SS) and incorporating perovskite layer between them via a one-step solution process. The coaxial fiber devices achieved efficiency of 3.3% and the photovoltaic parameters (Voc, Jsc, and FF) remained almost constant under different incident light angles. No damage was observed on the sheet electrode and the energy efficiencies remained at 95% after bending for 50 cycles. With two-step solution process, the corresponding perovskite fiber solar cells based on ZnO array achieved 3.8% efficiency[72].

Although the efficiency is only comparable with fiber inorganic and organic solar cells at present, the device performance are rather promising as initial trials. The above trials further confirm the openness of the fiber system to new photovoltaic types. Due to the excellent performance of perovskite solar cells, fiber perovskite solar cells have a great chance of catching up via further modification, and they might achieve equal or even higher efficiency than FDSCs. For practical applications, more research is needed to explore repeatable and scalable technology. But the perovskite layer is sensitive to moisture and hole transport material Spiro-OMeTAD [2,2',7,7'-tetraakis(N,N-di-p-methoxy phenylamine)-9,9'-spirobifluorene], suffer from de-doping process in the air, the stability and lifetime of fiber device need further improvement. Another drawback is the toxic elements, environmentally friendly alternatives are welcome. From this point of view, opportunities are there for novel photovoltaic types as well as fiber photovoltaics. In the ideal situation, reliable packages could help with the stability and pollution leakage problem at the same time. But some systemic work remains to be open before the scheme is acceptable.

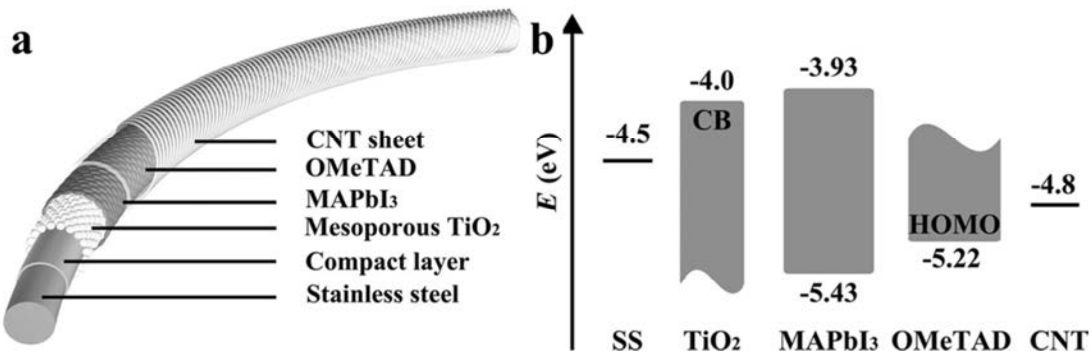

Figure 8 (a) Structure and (b) energy level diagram of flexible perovskite fiber solar cells based on carbon nanotube sheet[28]. Reproduced from Ref. 28 with permission, Copyright © 2014 WILEY-VCH Verlag GmbH & Co. KGaA, Weinheim.

As summarized in **Table 1**, fiber/wire-shaped solar cells, including inorganic, organic, dye sensitized, and perovskite, have made significant advancements. Fiber devices with length ≤ 5 cm were reported in most present literature. For high power output and weaving process, ultra-long, efficient and flexible fiber solar cells remain one of the most tempting challenges in this field. Compared with other fiber solar cells, FDSCs have achieved superior efficiency and larger device size. Moreover, FDSCs are easy and scalable to fabricate, as well as less sensitive to environmental factors. These advantages make them an attracting topic in material studies and achieve rapid progress.

Table 1 Photovoltaic parameters of typical fiber inorganic, organic, dye-sensitized and perovskite solar cells

Structure	Feature	*L* (cm)	*Jsc* (mA/cm^2)	*Voc* (V)	*FF*	*η* (%)	Ref.
CF/p-poly Si/n-poly Si/Ag	Hairlike single fiber	4	1.7	0.14	0.246	0.04	29
Capillary fiber/p-Si/i-Si/n-Si/Ti-Au	coaxial silicon fiber with p-i-n junction	1	2	0.22	0.55	0.5	30
Al-Pt/p-Si/i-Si/n-Si/ITO	silicon-core single fiber	<1	16.6	0.3	0.52	3.6	31
Mo/$CuInSe_2$/CdS/ZnO/ITO	Non-Si flexible fiber	4	13.0	0.34	0.522	2.31	27
Optical fiber/ITO/PEDOT:PSS/P3HT:PCBM/LiF/Al	Waveguide light-collection	~1.4	~7.0	/	/	1.1	32
SS/TiO_x/P3HT:PCBM/PEDOT: PSS/LiF/Ag/SS	ITO-free; twisted fibers; 5-30 cm	/	11.9	0.607	0.538	3.87	39
Ti/TiO_2/P3HT:PCBM/PEDOT:PSS/CNT fiber	flexible and stable	/	9.06	0.52	0.38	1.78	40
SS/ZnO/P3HT:PCBM/PEDOT:PSS/CNT yarn	CNT yarn; stable	/	8.49	>0.56	/	2.3	42
SS/ZnO/P3HT:PCBM/PEDOT:PSS/graphene	Single-layer graphene sheets	/	8.14	0.570	0.545	2.53	43
Ti/TiO_2/N719/I^--I_3^-/Pt	TiO_2 colloids; 3D light-harvesting	4.8	12.28	0.728	0.786	7.02	25
Ti/TMCA-TiO_2/N719/I^--I_3^-/Pt	Micron-core array; multilayer structure	5-7	16.04	0.702	0.717	8.07	54
Ti/TiO_2/N719/I^--I_3^-/graphene-Pt	Graphene/Pt composite fiber	/	/	0.744	0.63	8.45	58
Ti/TiO_2/N719/I^--I_3^-/TiN/carbon fiber	Helical photoanode; Non-Pt	/	19.35	0.64	0.58	7.20	59
Ti/TiO_2 nanotube/N719/I^--I_3^-/Pt	Flexible; ordered TiO_2 nanotube arrays	/	15.9	0.673	0.80	8.6	55
$(Ti/TiO2/N719)_6$/I^--I_3^-/Pt	Multi-fiber anodes	1.7	18.6	0.66	0.74	9.1	52
Ti/bilayer-TiO_2/N719/I^--I_3^-/Pt	Facile synthesis	5	/	/	/	Avg. 7.2	53
	Longest single device; highest power output	9.0	12.58	0.683	0.712	6.12	56
		31.5	8.09	0.716	0.692	4.01	56
CNT yarn /TiO_2/N719/I^--I_3^-/CNT yarn-Pt	Flexible; all carbon device	/	19.8	0.54	0.319	3.4	73

Optical fiber/ITO/TiO_2 NW/N719/I^--I_3^-/Pt	Waveguide; cylindrical electrode	2-3	18.50	~0.6	/	6	[74]
Ti/TiO2/N719/T^--T_2/CNT fiber	Flexible; non-I_2 electrolyte	/	15.49	0.683	0.69	7.33	[75]
SS/TiO_2/$CH_3NH_3PbI_3$/ Spiro-OMeTAD/CNT	Flexible coaxial perovskite solar fiber	<4	10.2	0.664	0.487	3.3	[28]
SS/ZnO/$CH_3NH_3PbI_3$/ Spiro-OMeTAD/CNT	ZnO nano-obelisk array; mild condition	<5	~12	~0.65	/	3.8	[72]

2 Properties of Fiber Solar Cells

Evolved from sandwich-type structure, the three dimensional structure endows fiber solar devices with special feature in light harvesting and charge transport, which further affects characterizations and applications. In principle, fiber solar cells with column symmetry should share similar properties. Since extensive studies of FDSCs have been well developed, we present the properties of fiber solar cells with FDSCs as a typical representative. In addition, compared with solid fiber solar cells, the liquid-based interfaces could relate to the high performance of FDSCs. Thus, we discuss the properties of fiber solar cells with focus on FDSCs in this part.

2.1 From Planar Structure to Fiber Style

FDSCs differ with typical and inverted DSSCs in composition, shape, flexibility, light collection, electron injection, and electrodes (**Table 2**). With Ti/TiO_2/Dye/electrolyte/Pt composition, FDSCs do not need TCO-based substrates, which are important in the total traditional DSSC cost. Different from traditional planar flat appearance, FDSC devices are in the form of wires, fibers, rods, or tubes; and flexible devices can be achieved by increasing the length/diameter ratio together with soft packages. These FSDC properties indicate a promising role in portable/wearable applications, which can be woven into flexible textiles. Since the utilization of high-melting-point fibers rather than polymer conductive substrates (e.g., ITO/PET, ITO/PEN)[76, 77], no temperature limitation exists during functional fiber preparation. Furthermore, given the symmetric cylindrical structure, FDSCs can harvest solar radiation in 3D space, more freedom than the front or back illumination (**Figure 9a** to **9d**)[25]. Experiments of various fiber solar cells have shown constant performance with different incident light angles[24, 28, 42]. Therefore, a simple diffusing plate under FDSC can improve light harvesting for higher power output via diffuse reflection illumination (**Figure 9e**). For example, power output could be greatly enhanced for fiber solar cells in conjunction with conventional rough substrates (e.g., foam board and white paper) and mirrors via light scattering and reflecting[50, 56, 78]. Nonetheless, reduced incident light in inverted DSSCs and FDSCs by electrolyte absorbance was observed compared with the light path of the front illuminated style. Reducing electrolyte thickness can lead to better solar energy harvesting. Under illumination, the photoelectrons from the excited dyes were injected into the conductive band of semiconductor layer and further collected through the current collector. The direction of electron injection in FDSCs and inverted DSSCs is along the incident direction, which is opposite to that of typical DSSCs. Furthermore, unlike DSSC and inverted DSSC cases, no explicit area/size ratio for the two electrodes is required, and they can be twisted together, packaged in parallel or film covered single fibers, which provide much freedom and convenience for structural design and material innovations. For fiber devices, the contact between electrolyte and sealing material is at two ends; smaller than that of the planar devices, which could reduce leakage rate. All these differences can essentially reflect the structure evolution from DSSCs to inverted DSSCs and further to FDSCs. And similar phenomena could exist in other types of fiber solar cells.

Table 2 Comparison of typical DSSCs, inverted DSSCs, and FDSCs

Type	**DSSCs**	**Inverted DSSCs**	**FDSCs**
Diagram	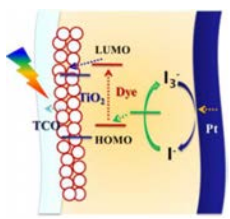	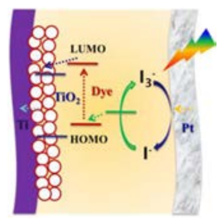	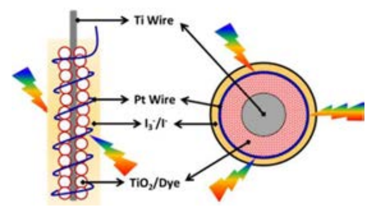
Composition	TCO/TiO_2/Dye/electrolyte/Pt/TCO	Ti/TiO_2/Dye/electrolyte/Pt/TCO	Ti/TiO_2/Dye/electrolyte/Pt
Shape	Flat	Flat	Wire/fiber/rod/tube
Flexibility	TCO substrate; area/thickness ratio	flexible substrate; area/thickness ratio	Soft package; length/diameter ratio
Light Collection	front illuminated; TCO→TiO_2/Dye	back illuminated; TCO/Pt →electrolyte→TiO_2/Dye	3D light harvesting; Tube→electrolyte→TiO_2/Dye
Electron Injection	Dye→TiO_2→TCO	Dye→TiO_2→Ti	Dye→TiO_2→Ti

Electrodes	Anode/Cathode=1/1; face-to-face	Anode/Cathode=1/1; face-to-face	No explicit ratio; twisted, in apparel or single fiber

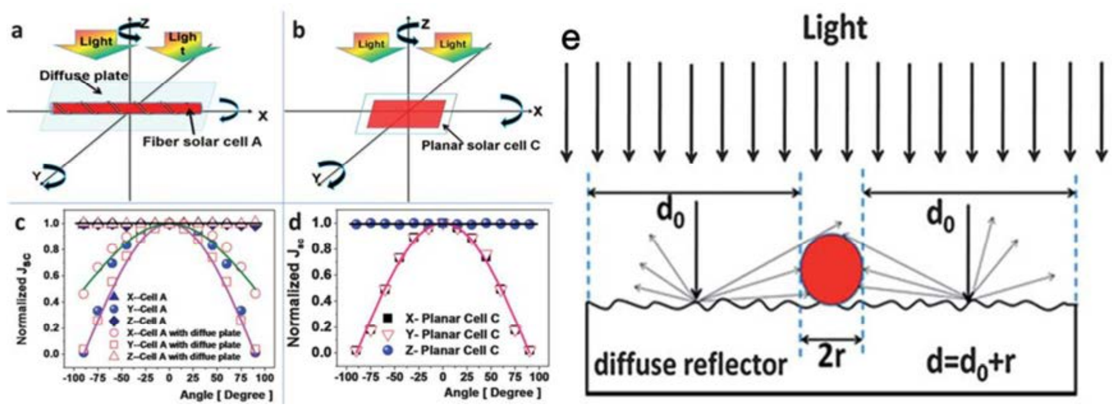

Figure 9 (a) 3D light-collecting schematic of the fiber-shaped solar cell (Cell A); (b) 3D light-collecting schematic of the traditional plate solar cell (Cell C); (c) the angle dependences of the normalized short-circuit currents of the Cell A and those of the composite Cell A; (d) the angle dependences of the normalized short-circuit currents of the plate Cell C. (e) Schematic of the diffuse reflection illumination mode[25]. Reproduced from Ref. 25 with permission from the Royal Society of Chemistry.

For flexible and wearable energy devices, the cohesion and adhesion of active layers would be crucial factors during textile manufacturing and weaving operations, as well as in maintaining device performance. Therefore, bulk fiber electrode with good conductivity and catalytic performance, like Pt wire, would be a good choice for the counter electrode. The dye-sensitized semiconductor oxides of the photoanode can form cracks upon deformation. Experiments have shown that damage induced by tensile deformation influence the device efficiency more than local damage, which indicates the practicability of preparing solar textiles from fiber devices, if the tension is well controlled[79]. Typically, thinner layer with good adhesion is preferable to prevent deep cracks, whereas thicker functional layer is preferable for higher efficiency[50, 53, 80]. A balance between flexibility and efficiency need further consideration of practical factors.

2.2 Characterization of Fiber Solar Cells

For typical sandwich-type solar cells, the illumination area is the apparent active area or masked geometrical area (**Figure 10a**). However, for fiber solar cells, only part of the photoanode is illuminated and the surface area of curved fiber is not the reasonable illumination area. According to the projection relation, the cross sectional area of the fiber photoanode is the position for direct solar energy harvesting (**Figure 10b**). Thus, in most recent works[50, 73, 81], the project area was used for efficiency calculation. The illumination area (A) is calculated as:

$$A = d * l$$

where d and l is the average diameter and effective length of fiber photoanode, respectively.

The short-circuit current density (Jsc) and the solar energy conversion efficiency (η) is calculated by:

$$J\text{sc} = I\text{sc}/A \text{ and } \eta = J\text{sc} \times V\text{oc} \times FF \times 100\%$$

Where Isc, Voc, and FF is the short-circuit current, open-circuit voltage, and fill factor, respectively.

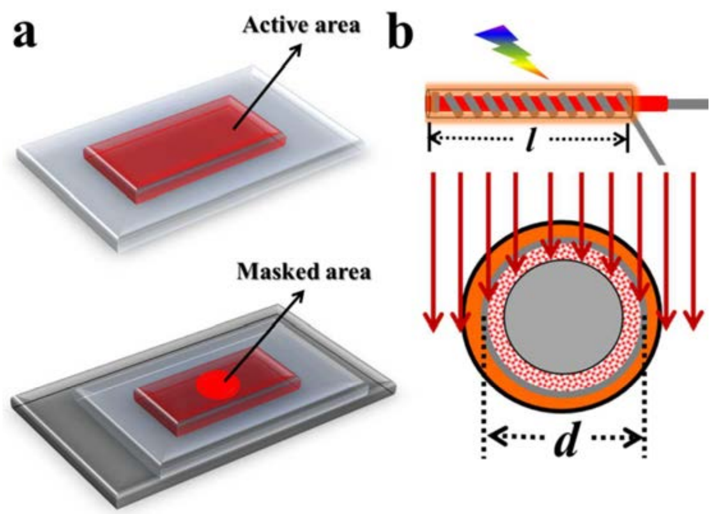

Figure 10 (a) The illumination area of typical sandwich-type solar cells is the apparent active area or masked geometrical area; (b) According to the projection relation, the cross sectional area of the fiber photoanode is the position for direct solar energy harvesting.

Photoanode with a smaller fiber diameter would lead to higher efficiency due to smaller active area under the same length[82], which indicates fiber substrates of micro/nanoscale might contribute to efficient devices. Notably, the size measurement (length and average diameter) error in short devices is larger than that in larger devices. Thus, device size should be considered in terms of measurement accuracy, as well as preparation difficulty, during efficiency comparison. For practical application and a more reasonable comparison with conventional DSSCs, the cross sectional area of the capillary tube is recommended to represent the cross section of the incident light[52, 82]. Reducing tube thickness and increasing its effective partial filling would benefit high-performance devices. Additionally, testing environment should be emphasized because of the 3D light harvesting property. Given the discrepancy of different voltage scanning directions, the average of the forward and backward tests is recommended as the final result for FDSCs[56].

Current literatures have dealt with the flexibility of fiber solar cells, but there is no uniform parameter as standard. The aspect ratio (the ratio of length and diameter), photovoltaic performance under various bending conditions (e.g. bending angles, bending radius, bending cycles), morphology after bending cycle(s), were typically experimental evidence for discussions.

2.3 Reasons for excellence of liquid-based FDSCs

To achieve efficient fiber solar devices, the key points are uniform functional layers and effective interface contact for efficient light collection, photoelectron generation, and charge transport. These points might be easier for traditional flat substrates, in which efficient solar cells have been fabricated. However, fiber substrates, which exhibit cylindrical surface and some uneven positions formed in the drawing process, may cause coating defects, layer fractures, and film perforation. These factors may exert significant adverse effects on thin film devices, such as invalid p-n junction, series charge recombination, or even short circuit. These problems become more pronounced in devices of large length and that is the reason why we emphasize device size in energy conversion efficiency comparison. Fortunately, a semiconductor oxide layer of more than 10 microns was enough to fill these grievances and cover the whole substrate in FDSC. Additionally, light collection can be weakened when the active layer is covered by a hole transport layer and/or outer metal current collector, which may limit photoelectron generation. Liquid electrolyte and twisted electrodes can mitigate this effect to a certain degree. Moreover, considering the interface contact, charge transfer at the solid-liquid heterojunction (photoanode/electrolyte interface) might be more efficient than that at solid-solid heterojunction. These are the possible reasons why FDSCs are currently more efficient than most other fiber solar cells. However, the possibility that real efficient solid-solid heterojunction would be discovered as evidence of technology development cannot be ruled out. In fact, higher current density short-circuit current (Jsc) or/and open-circuit voltage (Voc) can be expected in other solar cell types, even with lower fill factor (FF) than liquid-based FDSCs. We are quite optimistic that highly efficient solid fiber solar cells will be introduced in the near future.

3 Materials for FDSCs

3.1 Substrates

The substrate, which provides support to the whole device, is an important part of FDSCs. Mechanical strength, conductivity and specific surface area comprise the basic factors for fiber substrates. For flexible fiber devices, the aspect ratio of fiber electrodes determines FDSC flexibility. Therefore, flexible fiber substrates with smaller diameter and larger length would be ideal candidates for practical applications. Another challenge is that the weight and cost of fiber substrate should be as low as possible, and this is indeed a consideration for wearable applications. Conductive metal fibers, carbon-based fibers, polymer fibers, and optical fibers have been applied to FDSCs.

3.1.1 Metal Wires

Metal fibers are the most commonly used substrate for FDSCs owing to their good conductivity, mechanical strength, long-range flexibility, and high-temperature tolerance. Various metal wires[57, 82-84] including titanium, stainless steel, wolfram, aluminum, nickel, and zinc, have been utilized to collect photocurrent in the photoanode, as well as to support the whole device. Though started with stainless steel wire[24], most of the reported FDSCs and the most efficient FDSCs (7% to 9% efficiency) are fabricated with Ti-based photoanodes[52-55]. Annealing process of titanium wires can decrease the work function and increase Fermi level, which contributes to lower Schottky barrier[57]. However, W oxides formed during annealing leads to lower recombination resistance at the photoanode/electrolyte interface and results in lower open circuit voltage; the insulating Al_2O_3 and NiO layers, which could prevent the photoelectrons from being injected into the substrate (**Figure 11**), lead to poor efficiency[82, 83]. However, the above observations cannot exclude cheap metal substrate application for DSSCs because low-temperature-based process can avoid metal oxidation. However, active metals exposed to electrolyte may cause galvanic-battery reactions along with metal corrosion and oxidized species consumption, which eventually result in a non-functional device[85]. Therefore, covering the metal substrates via dense titanium oxide layer is a possible solution[57].

Moreover, cheap and light fiber substrates with titanium-coated layer may also play a role in high-purity titanium wire placement.

Furthermore, metal wires support the active catalytic components as counter electrodes in parallel with the photoanode[69, 86, 87]. Given the good conductivity, studying the electrochemical catalytic performance of new materials may be beneficial regardless of the impact of resistance.

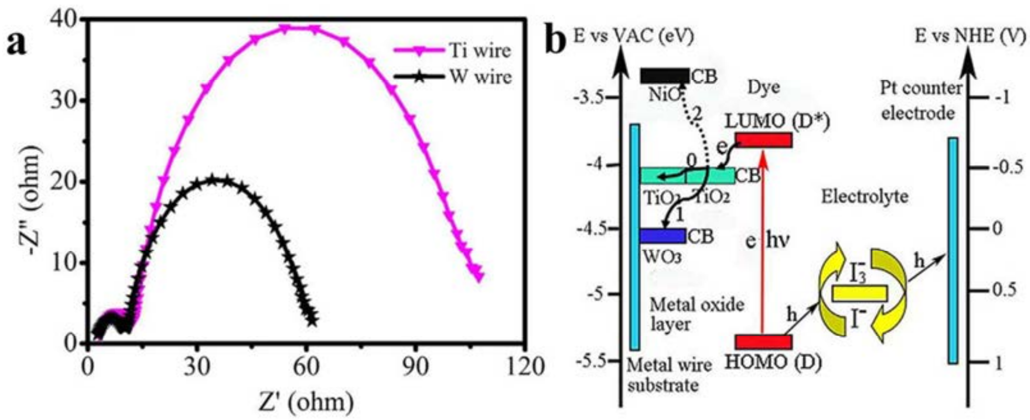

Figure 11 (a) EIS measurements for the FDSSCs based on W and Ti wires with TiO_2 photoanodes. The W based FDSCs showed a drastic decrease in the internal resistance, which means a larger recombination rate in photoelectrode, and which might be due to the high-level conduction band mismatch between the TiO_2 working electrode and the WO_3 layer. (b) Energy states diagram for different metal wire-based FDSC featuring the operation principle, and the dashed line shows the photoelectrons cannot transfer from TiO_2 nanoarray to NiO film[83]. Reproduced from Ref. 83 with permission, Copyright © 2014, Rights Managed by Nature Publishing Group.

3.1.2 Carbon-based Fibers

Carbon-based fibers are attractive candidates as electrodes for energy devices because of their salient flexibility, low density, high specific surface area, moderate conductivity, anti-corrosion property, and high strength[49, 88, 89]. Carbon fibers composed of micron-sized single fibers are commercial products and are utilized in FDSCs since 2011[90]. With even higher specific surface area, carbon nanotube (CNT) fibers based on nanosized monofilament were also applied in fiber solar cells by Peng's[91] and Cao's[92] groups. Core-sheath CNT/reduced graphene oxide (RGO) nanoribbon, CNT/RGO composite, and RGO fibers[93] (**Figure 12a**) benefit from the convenience of physical and/or chemical modifications, which bring more concept for materials science and device designs.

Carbon-based fibers can be used as supporters for dye-sensitized TiO_2 layer, such as nanoparticles, nanorodes (NRs), nanotube, and nanowires (NW)[60, 94, 95]. Wang et al. first demonstrated CF/TiO_2 NR array-based FDSC (**Figure 12b**) with efficiency of 0.76%; bunched-NR based device achieved higher efficiency of 1.28% because of higher Jsc attributed to the larger surface area[94]. FDSC with CF/TiO_2 NW photoanode obtained an impressive conversion efficiency of 2.48%[95]. The carbon fiber bundle diameter directly affects the device performance originating from the electrode conductivity, loading amount of dye-sensitized nano-TiO_2, and apparent device area[60]. Semiconductive CNT fibers were directly sensitized as photoanode, and the device packaged in the typical sandwich format achieved power conversion efficiency of 2.2%[91]. Nonetheless, these FDSCs are usually not self-standing, and additional substrate is required to support the device, which can be a problem for carbon-based fiber photoanode. Moreover, obtaining the accurate active area is not easy due to the disperse state in the electrolyte, and the apparent area in the dry state is used for efficiency calculation. However, these problems can be avoided when these fibers were used in the counter electrode.

Commercial carbon fibers consisting of single fibers were used as counter electrode or current collector in some innovative works, with efficiencies of 3.0% to 7.2% [59, 90, 96, 97]. A bunch of carbon fibers showed limited catalytic activity toward I_3^-/I^- redox couple, with 2.7% efficiency[25]. The structural defects on the nanotubes formed main catalytic sites for redox reactions by directly utilizing CNT fiber as the counter electrode, and 3.4% efficiency was reported[98]. The device performance showed some yarn diameter dependence because of the combination of active sites, conductivity, and electrode contact. With similar device structure, Peng et al. reported device efficiency up to 4.6% with CNT fiber[99] and 3.8% with graphene fibers[58]. CNTs can be rolled or twisted to fibers since they are usually grown as a thin film on planar substrate. To make advantage of the CNT thin films for device design, Cao et al.[92] reported single-wire DSSC (1.6%) via wrapping carbon nanotube film around the fiber photoanode (**Figure 12c**). Efficiency of 2.6% was achieved with the assistance of an Ag wire to overcome the CNT sheet resistance. Through film thickness optimization, similar coaxial structure offers a high energy conversion efficiency of 4.1% and stability during deformation[100]. These "CNT-enriched fiber solar cells" are attracting increasing attention given the attractive structures, moderate performance, and light weight[101-104].

A more challenge to single carbon-based electrode is the all-carbon based FDSCs reported from several groups, which employed carbon-based fibers as substrates of both electrodes (**Figure 12d**), thereby achieving 1.9% to 3.4% efficiency[60, 62, 73, 95, 105]. Even with non-liquid electrolyte, the all-carbon-based photovoltaic fibers photoconversion efficiency of 2.6% was achieved with all-carbon-based photovoltaic fibers, which is independent of incident illumination and cell shape or position[61, 106]. Despite the low efficiency, these works may provide a promising avenue toward lightweight and flexible solar cells.

The above results indicate that carbon-based fibers are promising materials for efficient FDSCs. However, the carbon-based fiber only is not enough for efficient charge exchange at the cathode/electrolyte interface, which resulted in relatively low *J*sc and *FF*. Thus, catalysts should be employed to avoid this restriction. In most cases, carbon-based fibers were used as supporting substrate because of their limited catalytic property but high specific surface area for additional chemical modifications. Various kinds of catalytic materials are discussed in Part 3.3.

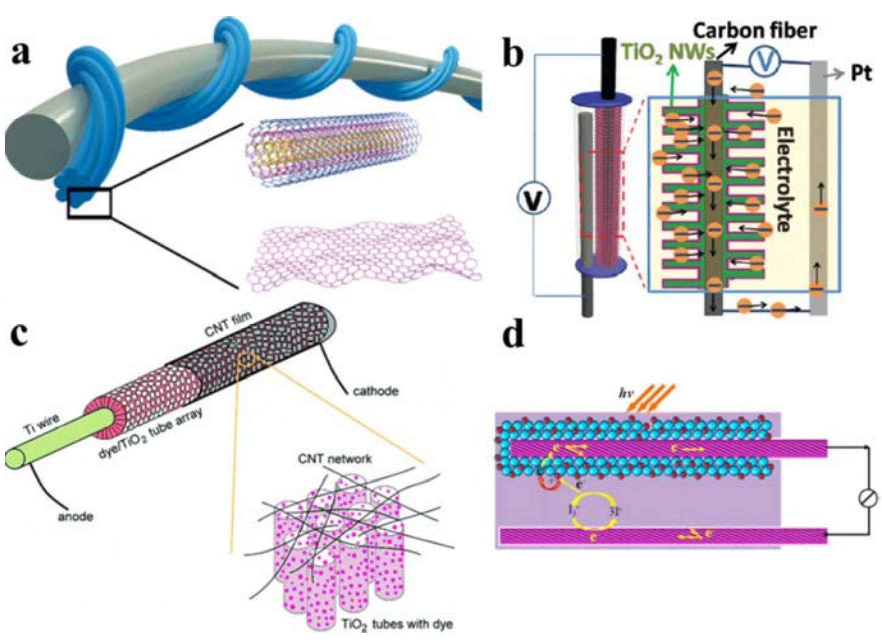

Figure 12 (a) FDSCs based on CNT and RGO fibers[93]. Reproduced from Ref. 93 with permission, Copyright © 2014, American Chemical Society. (b) Schematic of configuration of the CF/TiO_2 NR array-based tube-shaped DSSC[94]. Reproduced from Ref. 94 with permission, Copyright © 2012, American Chemical Society. (c) Flexible single-wire DSSCs by wrapping a carbon nanotube film around Ti wire-supported TiO_2 tube arrays as the transparent electrode[92]. Reproduced from Ref. 92 with permission, Copyright © 2011, American Chemical Society. (d) All-carbon-based FDSC with highly flexible aligned carbon nanotube fibers as catalytic counter electrode and current photoanode collector[105]. Reproduced from Ref. 105 with permission, Copyright 2012, American Chemical Society.

3.1.3 Polymer Fibers

Polymer fibers are flexible, lightweight, low-cost and commercially available materials, but not naturally conductive. The first challenge in practical electrochemical cell application is preparing conductive fiber substrates. Zou et al.[4] prepared flexible conductive threads on insulating thread substrates via dip-coating conductive PEDOT:PSS dispersion. The conductive threads showed good resistance to the solvents and achieved 4-5% efficiency as counter electrode in FDSCs (**Figure 13**). Fan et al.[107] reported Ni-deposited polymer materials as photoanode substrates for ZnO-based DSSCs, such as polybutylene terephthalate, polypropylene, polyethylene terephthalate, polyamide, and bio-mimetic veins. Lightweight DSSCs in the shape of wires, nets, and veins were fabricated via wet process.

Polymer fibers are raw materials for cloths, hats, and adornments. Polymer fiber-based energy devices may play a role in wearable electronics, which is one of the most important research motivations. Nevertheless, more efforts should be paid for better device performance and practical module design.

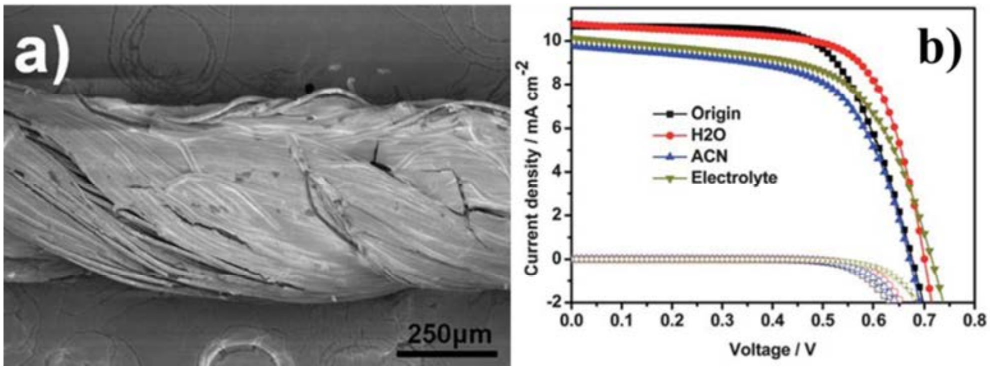

Figure 13 (a) Morphology of the conductive thread based on insulating thread substrates and PEDOT:PSS dispersion. (b) *J-V* curves of the fiber-shaped solar cells using conductive thread electrodes soaked in water, acetonitrile, and electrolyte, which corresponds to efficiencies of 4-5%[108]. Reproduced from Ref. 107 with permission from the Royal Society of Chemistry.

3.1.4 Optical Fibers

In 2009, Ferenets et al. designed a fiber solar device with optical fiber/ZnO:Al/TiO_2/N719/electrolyte/C, but its light harvesting was extremely hampered by the outmost carbon catalytic layer[109]. In the same year, Wang et al.[63] developed a hybrid photoanode with optical fiber/ITO/ZnO NW arrays for 3D DSSCs (**Figure 14**). The internal light reflection along the fiber expanded the opportunities for solar energy conversion, and the waveguide was extracted to the ITO/ZnO/Dye interface because of its higher refractive index. These FDSCs achieved an efficiency of 3.3%, and a corresponding efficiency enhancement factor (EEF) of 4.3 has been achieved by converting the 2D DSSC to the 3D DSSC. Additionally, by integrating optical fiber/ITO/TiO_2 NW hybrid fiber electrodes with the cylindrical counter electrode, an impressive efficiency of up to 6% has been demonstrated with EEF up to 9[74].

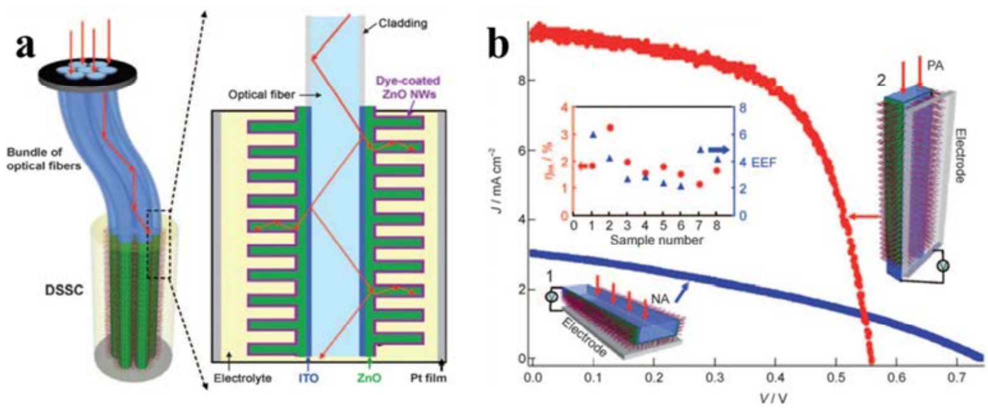

Figure 14 (a) A 3D DSSC was constructed based on ZnO NWs vertically grown on an optical fiber. The internal light reflection along the fiber was guided to the photoanode. (b) *J*-*V* curves of a DSSC under one full-sun illumination oriented 1) normal to the fiber axis (NA, 2D) and 2) parallel to the fiber axis (PA, 3D). A corresponding EEF of 4.3 has been achieved by converting the 2D DSSC to the 3D DSSC. The inset shows a plot of EEF and the corresponding energy conversion efficiencies for eight 3D DSSCs[63]. Reproduced from Ref. 63 with permission, Copyright © 2009 WILEY-VCH Verlag GmbH & Co. KGaA, Weinheim.

Given the special light harvesting characteristic via modified optical fibers, the direction of light reflected to the sensitized layer and photoelectron guided to the current-collecting electrode is similar to the cases in traditional planar DSSCs. Thus, ITO is involved as the transparent conductive layer on the fiber substrate. Moreover, the counter electrode can contribute to additional light reflection for solar energy harvesting especially in closed structures. Theoretical investigations have shown that DSSCs wrapped around an optical fiber can achieve as promising performance as standard geometry[110-112]. Some flexible or concentrating devices based on 3D solar cells may be expected in the future.

As previously mentioned, DSSCs can be assembled on various fiber substrates with quite high performance. With flexible FDSCs, photovoltaic braid can be woven as a network of single-fiber devices[56]. DSSCs with TCO-free flexible mesh substrate can also be treated as an extension to fiber-based photovoltaic devices[113-120], which are woven first and then applied as a device. Both approaches, which are similar in appearance, can play a role in future wearable electronics, but sealing small tubes with two ends is significantly simpler than flat plates[121]. Thus, apart from directly weaving the device, FDSCs with "down to the wire"[49] technology can provide opportunities for 3D devices, light-harvesting designs, and integrating innovations.

3.2 Semiconductor Materials for Photoanodes

TiO_2 nanoparticle with high specific surface area and good dye adsorption has been the basic material for porous fiber photoanode in early trials. Its suspension is a good candidate for dip-coating fiber substrates, with device efficiency of up to 7%[25, 50]. Considering the colloid preparation, in situ preparation of TiO_2 nanostructures on substrates is more convenient for device fabrications.

Electrons are more mobile by several orders of magnitude in 1D nanomaterials than in traditional nanoparticles, which could contribute to efficient FDSCs. Electrochemical anodizing of Ti wire substrates can lead to Ti-supported TiO_2 nanotube arrays, and the corresponding FDSCs achieved an efficiency of up to 7%[80, 122]. Electrolysis can be performed in large-scale preparation, and this process allows the fabrication of totally flexible devices. Surface treatment of TiO_2 nanotube arrays in niobium isopropoxide solution can weaken the electron recombination process and improve Voc and *FF*[123]. Transferring TiO_2 nanotubes to ordered hierarchical nanoparticles with NH_4F solution may result in an efficiency of 8.6% as demonstrated in a flexible FDSC with 30% improvement from the untreated group (**Figure 15**) [55]. Zhou et al.[124] synthesized TiO_2 nanowires array on Ti wire via $Na_2Ti_2O_5{\bullet}3H_2O$ NW trasformation in acid. For FDSCs, a high efficiency of 5.4% was achieved because of the high *J*sc. To simplify the preparation process, direct treatment of $Na_2Ti_3O_2$ network with $TiCl_4$ solution simultaneously exchanged Na^+ and formed a hierarchical structure[125]. Moreover, rutile TiO_2 NW or NR arrays were prepared on fiber substrates, but lower efficiency was achieved partly because of the suboptimal crystalline structure[94, 95]. After in situ preparations, an interstice between the Ti substrate and the oxidized layer is commonly observed. $TiCl_4$ post-treatment is advantageous in reducing the aforementioned defects and to the photoanode/electrolyte interface[80, 126].

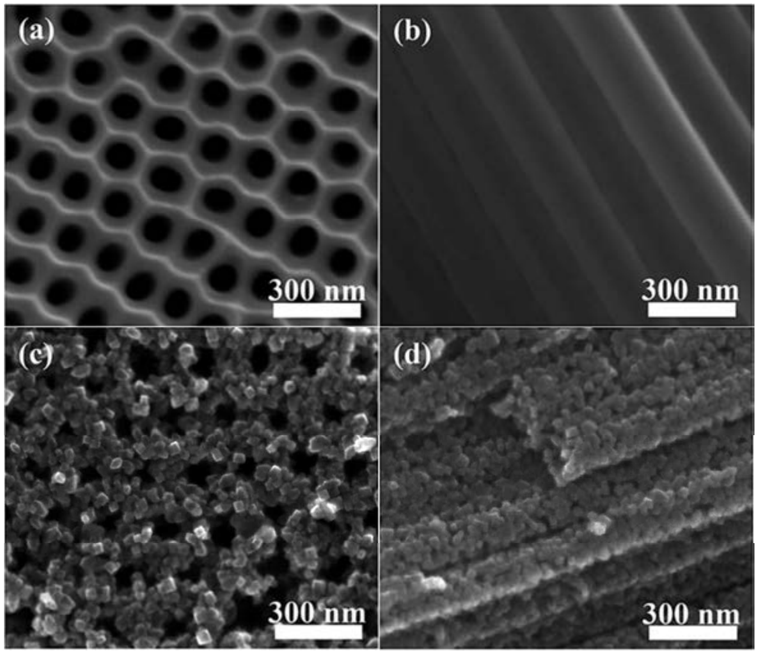

Figure 15 TiO_2 with different nanostructures for FDSCs: SEM images of a smooth TiO_2 nanotube array (a and b) and a hierarchical TiO2 nanotube array (c and d)[55]. Reproduced from Ref. 55 with permission from the Royal Society of Chemistry.

For better adhesion between the porous layer and the substrate, Zou et al.[53] reported facial synthesis via direct sintering of titanium tetraisopropoxide on titanium wire. FDSCs based on the compact layer exhibited an efficiency of 5.3%, and the high *FF*s indicated the good charge transport caused by the massive structure. To increase dye adsorption, the TiO_2 nanoparticle layer was dip-coated, and the FDSCs based on the bilayer structure achieved average efficiency of 7.2%. Compared with the device based on single nanoparticle layer, longer electron lifetime was obtained as a result of the reduced interface charge recombination. With the TiO_2 bilayer, 9-cm long flexible FDSC achieved an efficiency of 6.1% under AM 1.5 illumination and 11.4% with the assistance of a piece of white paper, and 80% of the efficiency was maintained after bending 180 times (**Figure 16**)[56]. Furthermore, for FDSCs, SnO_2-TiO_2 bilayer and trilayer structures were constructed via thermal calcination[127]. The J_{sc} enhancement derived by the SnO_2-TiO_2 junction and the recombination shielding effect of the compact TiO_2 film synergistically contributed to the high efficiency of 5.7%[127]. Additionally, TiO_2 micron-cone array via electrochemical reactions was used as the frame and electron transfer channel in fiber photoanodes. The TiO_2 multilayer structure composed of compact, light scattering, and porous layers was introduced into the fiber photoanode (**Figure 17**), and the fiber devices attained photoelectric conversion efficiencies of 7.6% to 8.1%[54]. The high performance implied the importance of designing multifunctional photoanodes. Nanoporous TiO_2 network as the inner layer contributed to better connection of the nanoparticle layer and Ti substrate, thus improving the electron transport rate and prolonging electron lifetime[126]. Aerosol spray pyrolysis was used for TiO_2-ZnO-based FDSCs, and computational fluid dynamic simulation could exhibit the flow field near the fiber substrate[128].

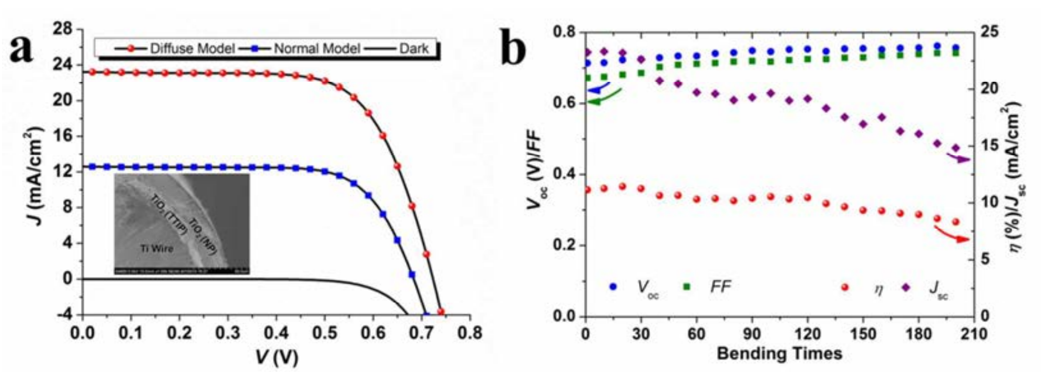

Figure 16 (a) *J-V* curves of the flexible FDSC (Length: 9.0 cm; photoanode diameter: 280 μm). The device was tested with a normal black background (normal model) and

with a sheet of A4 white paper as a diffuse plate (diffuse model). Inset: Ti supported TiO_2 bilayer structure. (d) Trend of photovoltaic parameters (Voc, FF, Jsc, and η) during the bending-recover cycles and the bending radius is approximately 3.0 cm[56]. Reproduced from Ref. 56 with permission from the Royal Society of Chemistry.

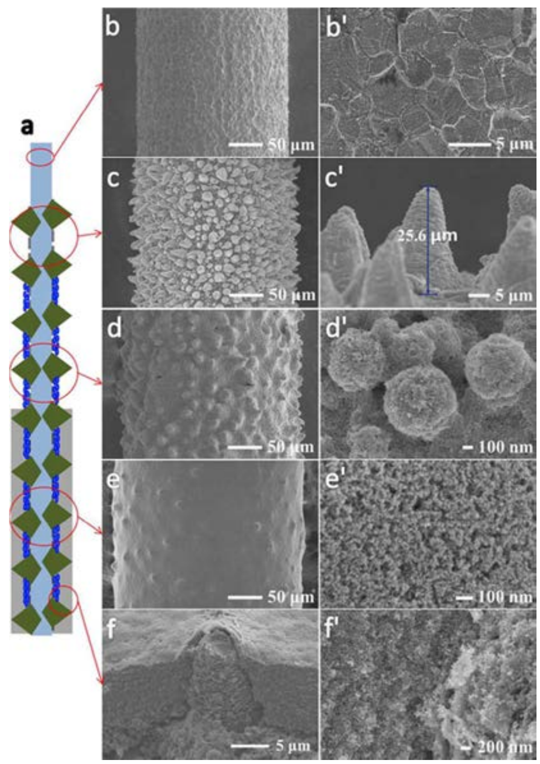

Figure 17 SEM images of the novel photoanode components.(a) the schematic drawing of the whole photoanode, (b) Ti wire treated by an acid mixture,(c)Ti/TiO2 micron-conearray, (d) light scattering layer, (e) porous layer, (f) cross section of the electrode; (b'), (c'), (d'), (e'), and (f') are the enlarged figures of (b), (c), (d), (e), and (f), respectively[54]. Reproduced from Ref. 54 with permission, Copyright © 2014 Published by Elsevier Ltd.

Recently, N3 and N719 are the most widely used dyes for FDSCs. To avoid the use of rare metal Ru, CdS and CdSe quantum dots (QDs) co-sensitized TiO_2 nanotubes for fiber solar cells obtained efficiency of up to 3.2% by optimizing the CdSe deposition time and the length of the nanotube[64]. A novel fiber solar cell with CdSe NW-grafted Ti wire achieved an efficiency of 2.9% in the S^{2-}/S_2^{2-} electrolyte[129]. The 1D solar cell on carbon fibers with vertical ZnO NWs and CdS QDs effectively absorbed visible light and converted it to electric energy[130]. Okoli and co-works[131] coated QDs-incorporated TiO_2 on CNT microyarn and intertwined it with a carbon nanotube microyarn. This carbon-based fiber solar cell achieved an efficiency of 5.9% with long-term stability. Additionally, CdS, CdSe, and N719 were incorporated in fiber photoanode (**Figure 18**) to realize both multiple exciton generation effects and multiple electron transmission paths. An efficiency of up to 6.4% was achieved, which may have resulted from the special anode design[78]. Thus, novel sensitizers may offer an access for further development. Based on QD solar cells, these fiber devices do not contain any rare metal or volatile electrolyte, making them cheap candidates for applications. However, the toxic metal Cd is a drawback in this approach.

Photoanodes demonstrate great potential for further development because of their multiple functions of light harvesting, photo-electron generation, and charge transport. New structures, materials, and synthesis routes for fiber photoanodes are still necessary, where more improvement could be expected.

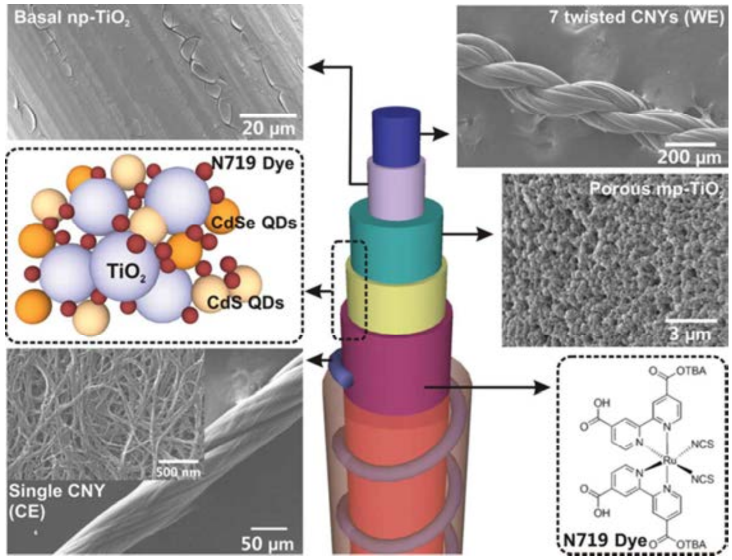

Figure 18 The wire-shaped CdS, CdSe, and N719 co-sensitized solar cell prepared by using a platinized CNY as counter electrode, a braid of 7-twisted carbon nanotube yarns with hybrid coating as the working electrode. Details are shown in SEM images and sketch maps[78]. Reproduced from Ref. 78 with permission, Copyright © 2014 WILEY-VCH Verlag GmbH & Co. KGaA, Weinheim.

3.3 Catalytic Materials for Counter Electrodes (Cathodes)

Pt is widely used as a counter electrode for DSSCs because of its good conductivity and good catalytic performance. Pt wire is the most common counter electrode for efficient FDSCs, reaching an efficiency of > 8 %[54, 55]. For cost considerations, the amount of Pt should be minimized. Decorating conductive fibers with Pt using various techniques, such as magnetron sputtering, electrolytic deposition, chemical reduction, and thermal pyrolysis, produced good results[58, 90, 97, 98]. Pt-decorated carbon fibers have exhibited improved conductivity and catalytic activity toward I_3^-/I^- redox couple than bare carbon fiber substrate, resulting in an FDSC efficiency of 5.8%[90].

FDSC based on Pt-CNT yarn achieved an efficiency of 3.7%, and annealing further improved efficiency to 4.8% because of the enhanced charge transfer across the Pt/CNT interfaces[98]. Superparamagnetic Fe_3O_4 and Ni nanoparticles were incorporated into CNT fibers for FDSCs, and they can stably attach to a magnet. Device efficiency of 6.0% was improved to 8.0% with Pt deposition[132]. Graphene/Pt composite fibers for FDSCs (**Figure 19a**) contributed to energy conversion efficiency of 8.5%[58].

To avoid rare-earth metal Pt, carbon-based materials, conductive polymers, and inorganic nanocomplexes were used for efficient FDSCs. In the early attempts, commercial pen ink based on well-dispersed carbon nanoparticles was proved to be good catalytic material for I_3^-/I^-- and T_2/T^-- based electrolytes. Ink-coated SS wires and carbon fibers in parallel with the photoanodes were applied in FDSCs (**Figure 19b**), and the optimal efficiency of 6.2% was achieved[133]. Nitrogen-doped graphene was also demonstrated as an efficient metal-free electro-catalyst for I_3^-/I^- redox couple.[86] Its pyridinic and quaternary nitrogen states especially provided active sites for promoting I_3^- reduction. For FDSCs, the nitrogen-doped graphene catalyst prepared under 900 °C achieved an energy conversion efficiency of 5.4%, comparable with Pt-based device under similar conditions. Further study indicated that conductive polymer PEDOT: PSS composite-coated carbon fiber electrode showed catalytic performance and long-term stability that were superior to those of Pt-decorated carbon fiber[96]. As the coating time (layer thickness) increased, the improved conductivity and catalytic performance of the fiber electrode realized a device efficiency of up to 5.6%. Polyaniline via in situ electrochemical polymerization displayed almost equivalent catalytic activity with SS sputtered with Pt, probably because of its porous characteristic and larger surface area. With this counter electrode, FDSCs achieved an efficiency of 5.4%[69]. Inorganic components are also good candidates for the fiber counter electrode. Porous, single crystalline titanium nitride (TiN) nanoplates were grown on carbon fibers via TiO_2 transfer[59]. Contrary to the typical design, the catalytic fiber was surrounded by helical photoanode (**Figure 19c**), and an efficiency of 7.2% was achieved in the FDSC with high *J*sc of 19.35 mA/cm^2. The intrinsic electrochemical properties, electrical conductivity of the TiN nanoplates, and their specific nanostructure (e.g., active sites, large macro-pores, tight fusion connectivity, and vertically aligned configuration) may function jointly for the photovoltaic performance. $CoNiS_2$ nanoribbon and NR on carbon fibers with good catalytic activity to I_3^-/I^- redox couple were applied to FDSCs (**Figure 19d**). The former achieved higher efficiency (7.0%) than the latter (4.1%). The distinct morphologies and exposed crystal facet are responsible for the significant distinction in performance[134].

Given that the functional electrode provides the current cycle, the counter electrode is of equal importance in the photoanode. Given the relatively simple electrochemical process, this fiber electrode is a good platform for traditional and new material studies. In response to the reduction reaction, a catalyst is necessary to reduce the over-potential and charge transport resistance. The size/amount of counter electrode is relatively unrestricted in FDSCs, non-Pt counter electrodes can reasonably “win” over

Pt by larger amount and/or higher specific surface area, except for the catalytic activity. Lighter weight, tighter connection, and smaller diameter are preferable for portable/wearable applications. Thus, materials with excellent catalytic activity, high specific surface area, long-term electrochemical stability, good adhesion, low cost, and easy preparation can play remarkable roles for efficient FDSCs.

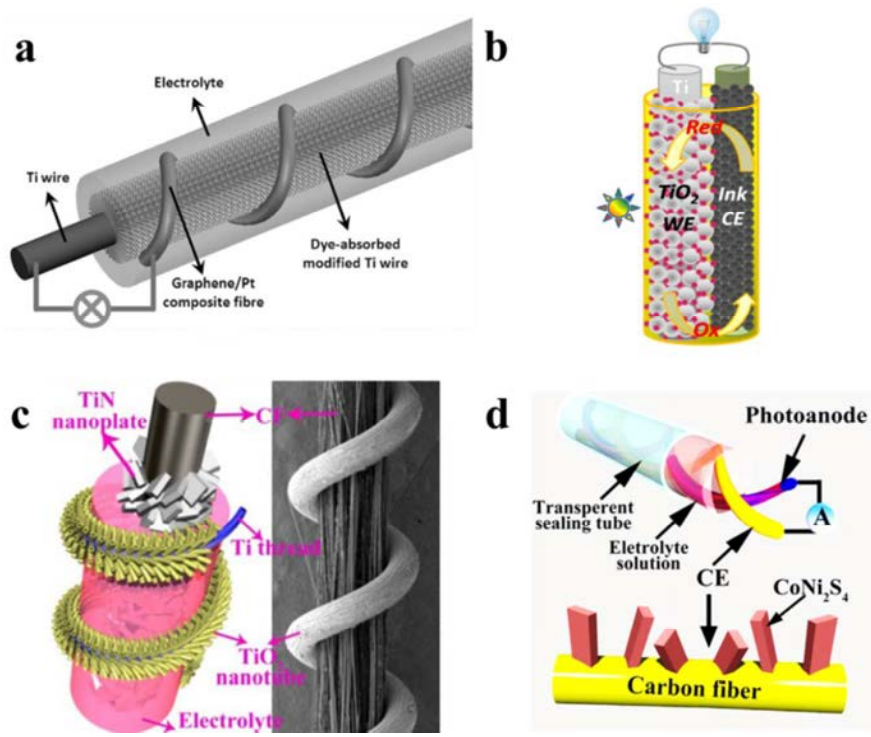

Figure 19 FDSCs based on various catalytic materials. FDSCs with (a) spiral-winded graphene/Pt composite fiber as counter electrode[58]. Reproduced from Ref. 58 with permission, Copyright © 2013 WILEY-VCH Verlag GmbH & Co. KGaA, Weinheim. (b) Parallel fiber electrodes and the commercial fountain pen ink as catalyst on the counter electrode[133]. Reproduced from Ref. 133 with permission from the Royal Society of Chemistry. (c) TiN nanoplate-functionalized CFs were twisted with the TiO_2 nanotube array-coated Ti thread for FDSCs[59]. Reproduced from Ref. 59 with permission from the Royal Society of Chemistry. (d) FDSCs based on $CoNi_2S_4$

nanoribbon- and NR-modified carbon fibers[134]. Reproduced from Ref. 134 with permission, Copyright © 2014 Elsevier Ltd.

3.3 Electrolyte

3.3.1 Liquid electrolyte

Liquid electrolyte based on I_3^-/I^- redox couple is the most used electrolyte for efficient FDSCs. The effects of I_2 concentration on the device performance are caused by two contradictory factors: light harvesting and charge transportation. Optimized I_2 concentration would balance these factors. Higher I_2 concentration indicates guaranteed charge transfer at counter electrode but more serious incident light loss. For concentrating systems, solar energy is excessive, and higher I_2 concentration is preferable for enhanced charge transfer at the counter electrode[68]. When the electrolyte in FDSCs is refreshed[135], the increased Voc is mainly ascribed to the electron recombination resistance at the photoanode/electrolyte interface, in which Li^+ was proved to play an important role. The desorption of sensitizers and the increase in series resistance during the dynamic process result in decreased Jsc and η.

Non-iodine electrolyte thiolate/disulfide (T_2/T^-) couple redox shows negligible absorption in the visible region, which would benefit light harvesting in FDSCs. Determining suitable catalytic materials for the redox couple is important toward the fabrication of an efficient device. Zou et al.[133] reported that pen ink/carbon fiber electrodes possess good catalytic activity toward T_2/T^- and contributes to achieve solar conversion efficiency of 4.0%, which is higher than that of Pt-based devices

(3.3%). Peng et al.[75] reported CNT counter electrode for flexible device with efficiency of 7.3%. Compared with core-sheath CNT/RGONR, CNT/RGO composite, and RGO fibers, the CNT fiber displays higher catalytic activity toward thiolate/disulfide couple redox and superior device performance[93].

Conventional liquid-based electrolytes have contributed to the most efficient FDSCs, but leakage and volatilization of the organic solution are potential long-term problems. Additional sealing is used to resolve this drawback in FDSC archetypes[136]. In this case, volatile solvents would be avoided in electrolytes in future photovoltaic applications. However, the liquid electrolyte can guarantee moderate charge transport and light transparency, which are important in the development of highly efficient FDSCs. These characteristics are suitable supporting conditions for electrode material and interface studies.

3.3.2 Gel electrolyte

Gel electrolyte, which is easy to prepare and coat, may be more advantageous for practical applications. Polymer-based network can provide passageway for the charge transport between two fiber electrodes, and the device performance has been gradually enhanced in recent studies. Zou and Wu's group first reported a poly(ethylene glycol) gel containing I_3^-/I^- redox couple for quasi-solid FDSCs, and an efficiency of up to 1.5% was achieved for TNT-based device[65]. Kang et al.[137] prepared porous polyimide films as separator for FDSC using the phase inversion technique. Additionally, they prepared a series of porous polymer electrolyte membranes of PVdF-HFP with various P123 contents. The photovoltaic fibers exhibited the optimal performance of 1.0%, and they were woven into mesh-like modules[138]. Although reported as a solid[106, 139, 140], treating the PVdF-HFP/3-MePRN/TBP composite as a gel may be more advantageous. The refreshed efficiency of 6.4% (7.4% with a mirror) and high Voc up to 0.8 V indicate the interface corporation of fiber anode with the electrolyte. Ionic salts possess good conductivity and low vapor pressure, and they can also avoid solvents. Peng et al. claimed an efficiency of 2.6% with eutectic melts of ionic salts, and the devices showed higher thermal stability and lifetime than liquid based FDSCs (**Figure 20**)[67, 141].

Thus, FDSCs based on gel electrolytes have achieved some progress, while further improvements may be performed. Recent gels derived from the traditional DSSCs can suffer from serious light absorption for FDSCs, which is responsible for the low Jsc and η. Exploring "more transparent" gels with good charge transport may be a solution.

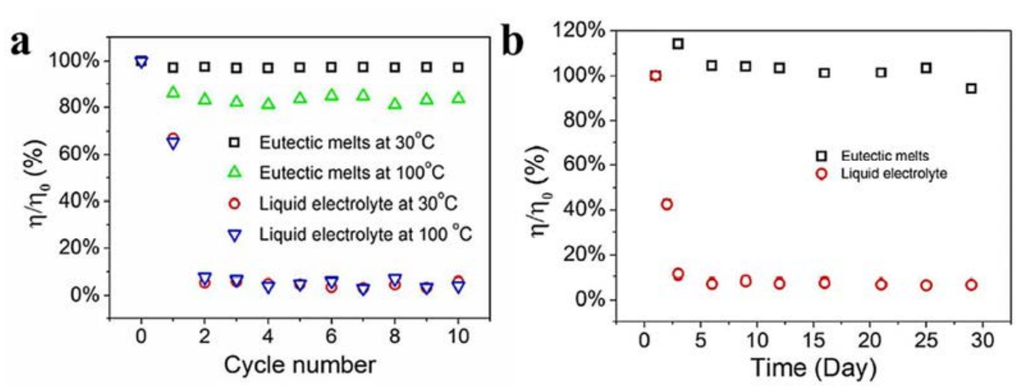

Figure 20 (a) η/η_0 values at 30 ºC and 100 ºC. FDSCs were repeatedly heated to 100 ºC and then cooled down to 30 ºC. η and η_0 correspond to the energy conversion efficiencies of the as-fabricated FDSC and the one after heating treatment. (b) Comparison on the operation stability of FDSCs based on liquid electrolyte and

eutectic melts. η and η_0 correspond to the energy conversion efficiencies of the as-fabricated FDSCs and the one in the following time during use. The devices were kept in dark at a temperature range of (25 ± 5) ºC and humidity range of (40 ± 30)%[141]. Reproduced from Ref. 141 with permission from the Royal Society of Chemistry.

3.3.3 Solid electrolyte

Solid electrolyte for FDSCs involves stable, solvent-free, and transparent film with good charge transport. Suitable hole-transport materials can avoid liquid linkage problem and provide long-term stability. But alternative materials for this case are very limited and preparing this functional layer is quite challenging.

In 2008, Zou et al. first applied CuI as the solid electrolyte for flexible FDSC, but the efficiency was only 0.06%[66]. The defects in the CuI layer on the curved surface probably affected the carrier mobility and limited the photovoltaic performance. The TNT-based photoanode contributed to the higher efficiency of 0.21%, and the remarkably improved carrier-transfer is the possible reason[65]. Additionally, flexible solid FDSCs with efficiency of 1.38% were fabricated by employing annealed Ti substrate and polymer-templated photoanode. The passivation layer formed on the substrate reduced the Schottky barrier at the anode interface. The micron holes increased the filling of the CuI electrolyte, which resulted in improved electron lifetime[57].

The solid FDSC presents a possible approach toward “dry” photovoltaic fiber as well as inorganic, organic, and perovskite fiber solar cells. Given the aforementioned severe requirements, limited choices of materials are available. Even the famous hole transport material Spiro-OMeTAD was not reported for solid FDSCs, probably because of the difficulty in preparing a uniform film of this material on a curved surface and its long-term stability in the air. Novel hole transport layers may be the key point for efficient solid FDSCs.

4 3D Solar Devices with Light-harvesting Designs

FDSCs can harvest solar energy from spatial sources because of the symmetrical structure of the fiber photoanodes. Special optical designs may be drawn on two levels: the individual fiber electrode and the fiber device itself. Light-harvesting designs were involved in power output maximization of a single device, as well as taking advantage of the active materials and fiber solar cell properties.

In a typical FDSC architecture, a Pt counter electrode twisted around the photoanode can hinder the incident light to the photoanode and the shading effect of electrolyte. Turning the two fibers around can avoid the problem and minimize the amount of Pt. Liu et al.[142] reported a mini 3D solar device (**Figure 21a**) utilizing a spiral-shaped Ti/TiO_2/N719 photoanode around the counter electrode with an energy conversion efficiency of 4.1%. Under natural sunlight, the modules with tree-like structure exhibited an efficiency of up to 4.9% with 3D light utilization[143]. Moreover, DNA-like DSSCs with symmetrical double-helix fiber photoanode and cathode were investigated (**Figure 21b**)[144, 145]. With spiral wire photoanode, a novel stretchable photovoltaic device was fabricated on elastic conductive rubber fibers twisted with CNT fiber (**Figure 21c**). The photovoltaic devices achieved an energy conversion efficiency of 7.1%, and the efficiency was well maintained under bending and stretching, which are important in portable electronic devices and facilities[146]. For 3D DSSC design, mesh-based photoanodes have also been applied to TCO-free cylinders with efficiency of 5.5%[147, 148]. These devices can capture light effectively from any direction to the device center. However, excess liquid electrolyte filled between electrodes in the sealing tube[149]. To reduce the amount of electrolyte, Hayase et al.[150, 151] designed coil-type TCO-less cylindrical DSSCs based on metal wire-supported TiO_2 porous layer with an efficiency of 3.9% to 4.7%. A glass mesh was employed to avoid potential short-circuit between the two packing electrodes. TiO_x layer formed on the wire, and the wire diameter affected the overall device performance. Considering the difficulty in preparing spiral dye-sensitized photoanodes and fixing electrodes, the above 3D architectures have not been paid much attention. However, opportunities are open for highly efficient and practical designs. Jia et al.[52] fabricated a flexible 3D solar device (**Figure 21d**) with multi-working electrodes and one counter fiber electrode, which further extended the 3D light-harvesting property of single fiber photoanode. The energy conversion efficiency increased gradually from 2.8% to 6.6% as the number of photoanodes increased from 1 to 6. Interface modification with Nb_2O_5 energy barrier refreshed the efficiency to 9.1%, which was retained about 93% under bending with different angles (1.7 cm-long device bended at 30^o, 90^o and 180^o).

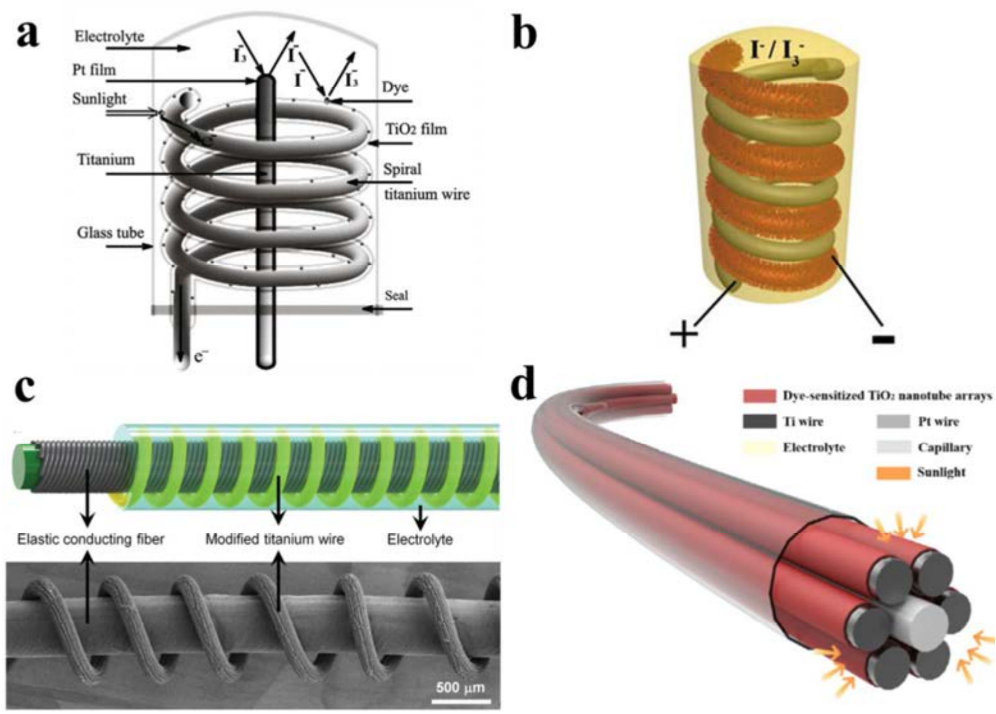

Figure 21 Typical structures of 3D FDSCs. (a) DSSCs utilizing spiral-shaped fiber photoanode around the counter electrode[143]. Reproduced from Ref. 143 with permission, Copyright © 2009 Elsevier Ltd. (b) Symmetrical double-helix fiber electrodes for DNA-like DSSC[144]. Reproduced from Ref. 144 with permission, Copyright © 2009 Published by Elsevier B.V. (c) Stretchable photovoltaic device based on spiral wire photoanode and elastic rubber fibers twisted with CNT fibers[146]. Reproduced from Ref. 146 with permission, Copyright © 2014 WILEY-VCH Verlag GmbH & Co. KGaA, Weinheim. (d) flexible 3D solar device with multi-working electrodes and one counter fiber electrode[52]. Reproduced from Ref. 52 with permission. Copyright © 2015 Elsevier Ltd.

With efficient fiber electrodes, TCO-free, flexible, and bifacial DSSCs (**Figure 21a**) were constructed with an efficiency of up to 2.4% (1.5 cm^2), which is quite different from that of traditional sandwich-type flat-cell structure[152]. Similar solar devices were realized based on dye-sensitized ZnO arrays[153] and multi-color solar textile was fabricated with metal-free organic dyes[154]. A flexible polymer solar cell textile with similar light-harvesting function was also developed. Ti/TNT mesh, which was coated with P3HT:PCBM and PEDOT:PSS layers, was adhered to transparent CNT sheets on both sides. The solid, lightweight, and flexible device exhibited an energy conversion efficiency of 1.1%[155].

Given the 3D light-collection property of fiber devices, the power output of FDSCs can be remarkably larger via catoptric and concentrated light. In 2011, Zou and co-workers[25] reported concentrating designs of FDSCs in conjunction with microgrooves (**Figure 22b**), including V-shaped, semi-ellipse, semicircle, and parabolic light condensers. In the parabolic groove, the converged light was theoretically perpendicularly to the FDSC and significantly increased the output power by fivefold. Similar result was confirmed by Jia et al[125]. To overcome the absorption of electrolyte, red-shift the incident light is a proper solution, but solar energy losses during the luminescence. Luminescent solar concentrators can down-shifting and concentrating light at the same time and could play a role in fiber solar designs. Integrating FDSCs and luminescent solar concentrators via grooves (**Figure 23**), semi-transparent and colorful waveguide solar devices were achieved, which may be used as solar windows[68, 156]. The effects of concentrator selection, device design, iodine concentration, illumination area, angle of inclination, and light intensity were analyzed. Maximum output power achieved an enhancement factor of

5.7 via efficient light collection over a large area.

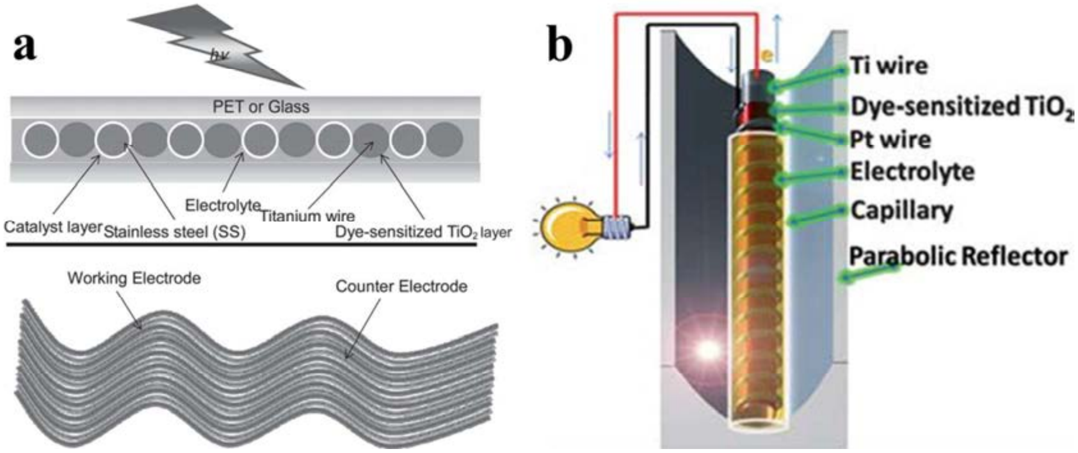

Figure 22 (a) Cross section (up) and sketch (down) of the flexible bifacial DSSC[152]. Reproduced from Ref. 152 with permission, Copyright © 2012 WILEY-VCH Verlag GmbH & Co. KGaA, Weinheim. (b) FDSCs in conjunction with microgrooves[25]. Reproduced from Ref. 25 with permission from the Royal Society of Chemistry.

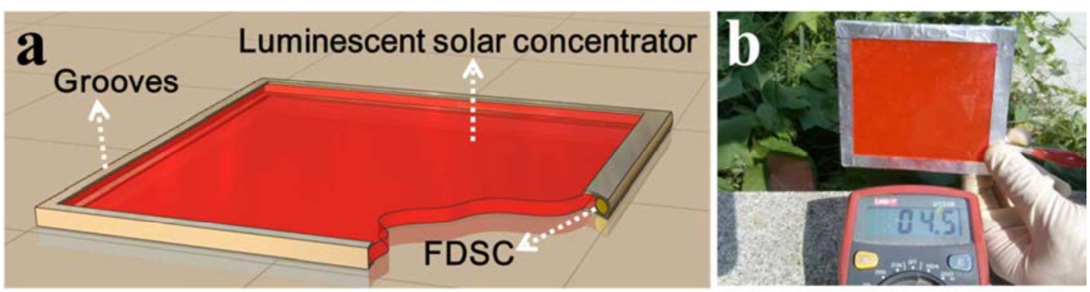

Figure 23 (a) The scheme of waveguide solar devices integrating FDSCs and luminescent solar concentrators via grooves[68]. Reproduced from Ref. 68 with permission from the Royal Society of Chemistry. (b) Waveguide devices with nearly 90^{o} tilted angle achieved *I*sc of 4.5mA under natural light illumination (14:11-14:17 on September 11th, 2013)[156]. Reproduced from Ref. 156 with permission, Copyright © 2014 Elsevier Ltd.

5 Fiber Hybrid Energy Systems for Flexible Electronics

Solar energy is widely distributed and environmentally friendly, but the weather and night can break its continuous supply. For flexible energy management, combining solar energy conversion with electrical power storage is a reliable approach. The power fibers are lightweight, flexible, and scalable, and they can be easily integrated into electronic textiles. Integrated fiber-shaped energy devices can serve as a solar-powered system for portable microelectronics, which significantly improved the original scope of photovoltaic cells and resulted in extensive opportunities for interdisciplinary research.

Considering the wire shape, integration of fiber solar cells with fiber shaped supercapacitors (FSCs) has attracted much attention[157]. In 2011, Wang and co-workers[26] considered the integration of multiple energy harvesters and a storage device along a single fiber. In their design, a nanogenerator, DSSC, and supercapacitor were built on a flexible PMMA fiber coated with thin Au film (**Figure 24a**). However, these devices were characterized separately, and the incorporation of multi-energy conversion approaches was not presented. Zou et al.[69] developed an integrated power fiber with overall efficiency of 2.1% that incorporated FDSCs and FSCs (**Figure 24b**). The polyaniline-coated SS wires acted as the counter electrode of FDSCs (5.4%) and symmetrical electrodes of faradic supercapacitors (19 mF/cm^2). Peng et al.[70] applied CNT fiber for FDSC (2.2%) and double-layer supercapacitors (0.6 mF/cm^2), and the integrated system exhibited an overall efficiency of 1.5%. These trials successfully used the catalytic and electrochemical properties of multi-functional materials, and attempts toward gel/solid single integrated power fibers are promising. Ti wire-supported titania nanotubes and aligned CNT sheet are two electrodes for both FDSCs and supercapacitors[158, 159]. These bi-functional devices achieved maximal solar energy conversion efficiency of 6.58% and specific length capacitance of 85.03 mF/cm, respectively[158]. With solid electrolyte, the photoelectric conversion and energy storage efficiencies have reached 2.73% and 75.7%, respectively[159]. The overall device efficiency was maintained by 88% after 1000 bending cycles and by 90% after 1000 hours. With similar design, organic fiber solar cells have also been utilized to the integrated system (**Figure 24c**)[160]. The organic solar cell based on P3HT: PCBM and PEDOT: PSS layers achieved an efficiency of 1.0% and an asymmetrical supercapacitor energy storage efficiency of 65.6%. The all solid-state and self-powered fiber showed an entire solar-electrical conversion efficiency of 0.82%.

In addition to the above linear localized power fibers, coaxially integrated power fibers were also designed for multi-step energy conversion. A coaxial energy fiber integrating 3D solar cell in its sheath and CNT double-layer supercapacitor in the core was developed (**Figure 24d**)[161]. This energy fiber exhibited a total efficiency of energy conversion and storage of 1.83%. The coaxial structure and aligned nanostructure at the interface of the electrode enabled the device to be robust to bending and stretching. These characteristics facilitate the practical application of these devices on wearable electronics.

Although characterized with high power output, FSCs with low energy density would become saturated after solar-charging for only several minutes. Thus, a fiber rechargeable battery may be more suitable for long-term energy storage. Zou et al. developed a flexible fiber-shaped zinc bromide battery with capacity of up to 19 mA h/mL and energy efficiency of 69%. This battery exhibited good cycle stability, linear capacity, and linear energy density. The design included flexible conductive electrodes without additional fragmenting coating layers. This characteristic enhanced the device flexibility and allowed the fiber battery to be easily integrated into the cloth for wearable electronics. Solar-charging the fiber battery with flexible fiber-based solar modules resulted in an overall efficiency of 3.4% for the hybrid energy system[56].

Fiber solar cells have been integrated to other hybrid energy systems. Wang et al.[162] demonstrated an optical fiber-based coaxially structured 3D compact hybrid cell (**Figure 24e**), in which the DSSC core harvested solar energy, while the piezoelectric nanogenerator shell harvested mechanical energy. The flexible device can work simultaneously or independently, and the output of the hybrid cell (~7.65 μA current and 3.3 V voltage) is strong enough to power nanodevices or even personal electronics.

Still, recent hybrid energy systems are in the preliminary stage. More concept than design art is expected, especially device scale, performance, repeatability, and cost, et al. As the evolution of device physics, multi-functional energy devices are on the way.

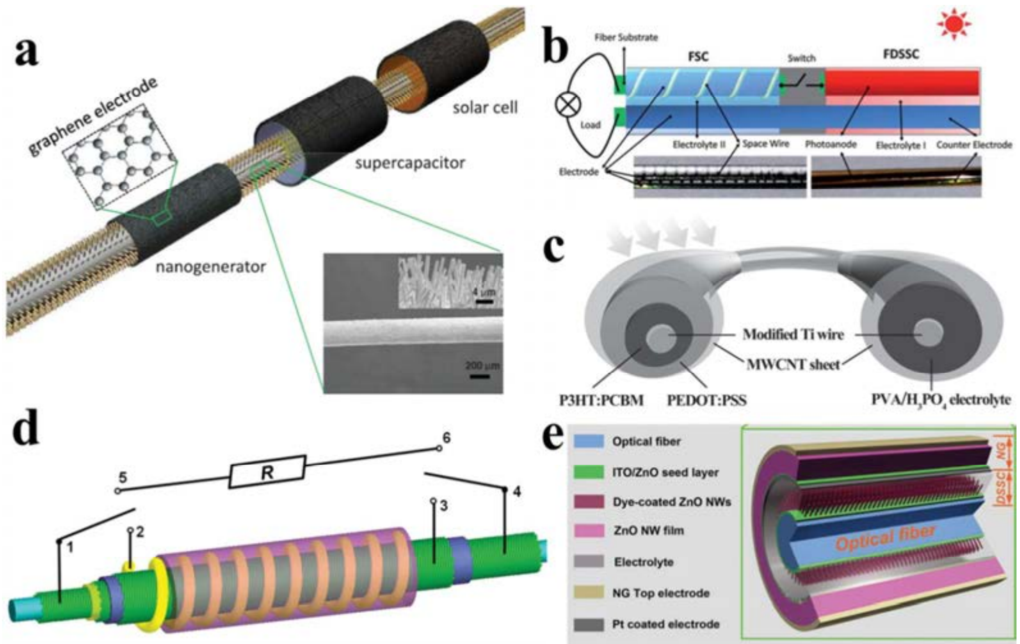

Figure 24 (a) Fiber-based multi-energy device composed of a nanogenerator, solar cell, and supercapacitor. ZnO NWs were grown on the Au-coated flexible plastic wire and Cu mesh with conductive graphene as electrodes[26]. Reproduced from Ref. 26 with permission, Copyright © 2011 WILEY-VCH Verlag GmbH & Co. KGaA, Weinheim. (b) Integrated power fiber consisting of an FDSC and FSC[69]. Reproduced from Ref. 69 with permission from the Royal Society of Chemistry. (c) All solid-state, coaxial, and integrated fiber devices based on organic fiber solar cell and supercapacitor[160]. Reproduced from Ref. 160 with permission, Copyright © 2013 WILEY-VCH Verlag GmbH & Co. KGaA, Weinheim. (d) Self-powered, elastic energy fiber with 3D solar cell in its sheath and CNT double-layer supercapacitor in the core[161]. Reproduced from Ref. 161 with permission, Copyright © 2014 WILEY-VCH Verlag GmbH & Co. KGaA, Weinheim. (e) The 3D hybrid cell with an optical FDSC, which harvests solar energy, and a piezoelectric nanogenerator shell, which harvests mechanical energy[162]. Reproduced from Ref. 162 with permission, Copyright © 2012 WILEY-VCH Verlag

GmbH & Co. KGaA, Weinheim.

Summary and Perspectives

Various fiber/wire-shaped solar cells have achieved great progress in recent years. Especially, the energy conversion efficiency of FDSCs has remarkably and rapidly increased from < 0.5% to > 9%. Moreover, ultra-long, flexible, stable, and lightweight devices have been reported as potential flexible/wearable power sources. However, these notable features were realized in different systems. For example, high efficiencies appeared without long-term stability and large size. Lightweight and stable devices were reported with relatively low efficiency or power output. Future explorations should be aimed at optimizing the device parameters and features synergistically.

Despite promising device performance, the liquid electrolyte is the potential drawback for FDSCs. Opportunities are open for quasi-solid and solid FDSCs, as well as other inorganic, organic and hybrid photovoltaic fibers. We believe that perovskite solar cells, which can be constructed via solution process, can be a suitable candidate for efficient solid photovoltaic fibers. Further material science, interface engineering and structural designs can promote perovskite solar fibers to higher levels, such as efficient perovskite solar wires in tens of centimeters, self-standing devices with harmless/protective packages, and solar textiles for wearable power sources. Beyond material science and fiber architectures, other considerations, such as technical solutions to controllable electrode disposition and efficient manufacture/integration, may be considered for actual solar textiles, which were discussed by Krebs et al[163]. But the particularity of fiber solar cells might bring new concept to the technical field.

The properties of fiber devices have been gradually recognized and utilized to optical designs for high power output. Replacement of rare-metal materials is another concern in previous studies, and satisfying results have been achieved. Novel materials and micro/nanostructure construction are the keys for these breakthroughs, and the foundation for further innovations has been established. The structure of fiber devices has also been extensively developed to flexible or even elastic 3D solar devices and integrated energy systems. Although previous studies only provided the initial ideas, they facilitated the breakthrough for novel solar architecture and portable/wearable electronics of the future.

We are optimistic that new materials, preparation technology, and interface engineering can make a difference in the future, and photovoltaic fiber will find its role as a solar technology. Further studies on fiber innovation may also result in higher efficiency, longer lifetime, harmless devices, practical solar modules, and solar-driven electronics, among others.

Acknowledgements

This study is jointly supported by Ministry of Science and Technology of China (No. 2011CB933300), Ministry of Education of China (No. 20120001140010), National Natural Science Foundation of China (No. 91333107), the fund from Shenzhen City (No. CXZZ20120618162051603) and Research Grants Council of the Hong Kong Special Administrative Region, China, SRFDP&RGC ERG Joint Research Scheme (No. M-HKBU209/12).

Photograph and biography

Ming Peng received his B.S. Degree in 2011 from Wuhan University, Wuhan, China. He is a Ph.D. candidate of Zou Lab in the Department of Polymer Science and Engineering, College of Chemistry and Molecular Engineering at Peking University. His main research interest is synthesis of optoelectronic nanomaterials and design of novel fiber based solar cells and batteries.

Dr. Dechun Zou received his doctoral degree from the Kyushu University, Japan, in 1990. He joined Mitsubishi Petrochemicals, Japan as a research scientist from 1990 to 1993, Tokyo University of Agriculture and Technology as a visiting researcher from 1994 to 1995, Casio Computer Co., Ltd. as a research contractor in 1996, CREST, JST (Tsutsui Project) as a research contractor in 1997. He was an associate professor in Kyushu University from 1998 to 2001. Since 2001, he has been a professor in the College of Chemistry and Molecular Engineering, Peking University, China. His research interests include organic light-emitting diodes, photovoltaics, flexible energy conversion/storage devices and related device physics. He was one of the recipients of the National Science Fund for Distinguished Young Scholars. At present, he is the chief scientist of National Key Basic Scientific Research Program on fiber-shaped solar cells in China.

References

1. M. A. Green, K. Emery, Y. Hishikawa, W. Warta and E. D. Dunlop, *Progress in Photovoltaics: Research and Applications*, 2015, **23**, 1-9.

2. T. K. Todorov, J. Tang, S. Bag, O. Gunawan, T. Gokmen, Y. Zhu and D. B. Mitzi, *Advanced Energy Materials*, 2013, **3**, 34-38.
3. http://www.nrel.gov/ncpv/images/efficiency_chart.jpg.
4. R. F. Service, *Science*, 2003, **301**, 909-911.
5. A. R. Köhler, *Materials & Design*, 2013, **51**, 51-60.
6. X. Wang, X. Lu, B. Liu, D. Chen, Y. Tong and G. Shen, *Advanced Materials*, 2014, **26**, 4763-4782.
7. L. Li, Z. Wu, S. Yuan and X. Zhang, *Energy & Environmental Science*, 2014, **7**, 2101-2122.
8. X. Cai, M. Peng, X. Yu, Y. P. Fu and D. C. Zou, *Journal of Materials Chemistry C*, 2014, **2**, 1184-1200.
9. K. Jost, G. Dion and Y. Gogotsi, *Journal of Materials Chemistry A*, 2014, **2**, 10776-10787.
10. M. B. Schubert and J. H. Werner, *Materials Today*, 2006, **9**, 42-50.
11. S. Wang, L. Lin and Z. L. Wang, *Nano Energy*, 2015, **11**, 436-462.
12. D. C. Zou, Z. B. Lv, X. Cai and S. C. Hou, *Nano Energy*, 2012, **1**, 273-281.
13. D. C. Zou, D. Wang, Z. Z. Chu, Z. B. Lv and X. Fan, *Coordination Chemistry Reviews*, 2010, **254**, 1169-1178.
14. T. Chen, L. B. Qiu, Z. B. Yang and H. S. Peng, *Chemical Society Reviews*, 2013, **42**, 5031-5041.
15. T. Könyves-Toth, A. Gassmann and H. von Seggern, *Materials*, 2014, **7**, 5254-5267.
16. S. Pan, Z. Zhang, W. Weng, H. Lin, Z. Yang and H. Peng, *Materials Today*, 2014, **17**, 276-284.
17. X. Wang, K. Jiang and G. Shen, *Materials Today*, 2015, DOI: 10.1016/j.mattod.2015.1001.1002.
18. D. Yu, Q. Qian, L. Wei, W. Jiang, K. Goh, J. Wei, J. Zhang and Y. Chen, *Chemical Society Reviews*, 2015, **44**, 647-662.
19. DE3209548-A, JP60042876-A, EP745276-A and JP8018080-A.
20. US2005211294-A1, JP2005216861-A and CN200610114454.7.
21. B. Baps, M. Eber-Koyuncu and M. Koyuncu, *Key Engineering Materials*, 2001, **206-213**, 937-940.
22. H. Kuraseko, T. Nakamura, S. Toda, H. Koaizawa, H. Jia and M. Kondo, *Photovoltaic Energy Conversion, Conference Record of the 2006 IEEE 4th World Conference on* 2006, **2**, 1380-1383.
23. J. Liu, M. A. G. Namboothiry and D. L. Carroll, *Applied Physics Letters*, 2007, **90**, 63501.
24. X. Fan, Z. Z. Chu, F. Z. Wang, C. Zhang, L. Chen, Y. W. Tang and D. C. Zou, *Advanced Materials*, 2008, **20**, 592-595.
25. Y. P. Fu, Z. B. Lv, S. C. Hou, H. W. Wu, D. Wang, C. Zhang, Z. Z. Chu, X. Cai, X. Fan, Z. L. Wang and D. C. Zou, *Energy & Environmental Science*, 2011, **4**, 3379-3383.
26. J. Bae, Y. J. Park, M. Lee, S. N. Cha, Y. J. Choi, C. S. Lee, J. M. Kim and Z. L. Wang, *Advanced Materials*, 2011, **23**, 3446-3449.
27. L. Zhang, L. Song, Q. Tian, X. Kuang, J. Hu, J. Liu, J. Yang and Z. Chen, *Nano Energy*, 2012, **1**, 769-776.
28. L. Qiu, J. Deng, X. Lu, Z. Yang and H. Peng, *Angewandte Chemie International Edition*, 2014, **53**, 10425-10428.
29. W. Xu, S. Choi and M. G. Allen, *Micro Electro Mechanical Systems (MEMS), 2010 IEEE 23rd International Conference*, 2010, 1187-1190.

30. R. He, T. D. Day, M. Krishnamurthi, J. R. Sparks, P. J. Sazio, V. Gopalan and J. V. Badding, *Advanced Materials*, 2013, **25**, 1461-1467.
31. F. A. Martinsen, B. K. Smeltzer, M. Nord, T. Hawkins, J. Ballato and U. J. Gibson, *Scientific Reports*, 2014, **4**, 6283.
32. J. Liu, M. A. G. Namboothiry and D. L. Carroll, *Applied Physics Letters*, 2007, **90**, 133515.
33. S. Chuangchote, T. Sagawa and S. Yoshikawa, *9th Eco-Energy and Materials Science and Engineering Symposium*, 2011, **9**.
34. B. O'Connor, K. P. Pipe and M. Shtein, *Applied Physics Letters*, 2008, **92**, 193306.
35. A. Bedeloglu, A. Demir, Y. Bozkurt and N. S. Sariciftci, *Textile Research Journal*, 2009, **80**, 1065-1074.
36. Y. Li, E. D. Peterson, H. Huang, M. Wang, D. Xue, W. Nie, W. Zhou and D. L. Carroll, *Applied Physics Letters*, 2010, **96**, 243505.
37. J. Hur, K. Im, U. J. Kim, T.-H. Kim, J.-J. Park, S. Hwang and N. Park, *Japanese Journal of Applied Physics*, 2014, **53**, 05HB01.
38. Y. Li, M. J. Wang, H. H. Huang, W. Y. Nie, Q. Li, E. D. Peterson, R. Coffin, G. J. Fang and D. L. Carroll, *Physical Review B*, 2011, **84**, 085206.
39. M. R. Lee, R. D. Eckert, K. Forberich, G. Dennler, C. J. Brabec and R. A. Gaudiana, *Science*, 2009, **324**, 232-235.
40. Z. Zhang, Z. Yang, Z. Wu, G. Guan, S. Pan, Y. Zhang, H. Li, J. Deng, B. Sun and H. Peng, *Advanced Energy Materials*, 2014, **4**, 1301750.
41. T. Chen, L. Qiu, H. Li and H. Peng, *Journal of Materials Chemistry*, 2012, **22**, 23655-23658.
42. D. Liu, M. Zhao, Y. Li, Z. Bian, L. Zhang, Y. Shang, X. Xia, S. Zhang, D. Yun, Z. Liu, A. Cao and C. Huang, *ACS Nano*, 2012, **6**, 11027-11034.
43. D. Liu, Y. Li, S. Zhao, A. Cao, C. Zhang, Z. Liu, Z. Bian, Z. Liu and C. Huang, *RSC Advances*, 2013, **3**, 13720-13727.
44. Z. Zhang, X. Li, G. Guan, S. Pan, Z. Zhu, D. Ren and H. Peng, *Angewandte Chemie International Edition*, 2014, **53**, 11571-11574.
45. S. Lee, Y. Lee, J. Park and D. Choi, *Nano Energy*, 2014, **9**, 88-93.
46. Y. Li, W. Nie, J. Liu, A. Partridge and D. L. Carroll, *IEEE Journal of Selected Topics in Quantum Electronics*, 2010, **16**, 1827-1837.
47. B. O'Connor, D. Nothern, K. P. Pipe and M. Shtein, *Optics Express*, 2010, **18**, A432-A443.
48. A. Hagfeldt, G. Boschloo, L. Sun, L. Kloo and H. Pettersson, *Chemical Society Reviews*, 2010, **110**, 6595-6663.
49. http://www.nature.com/nmat/journal/v7/n3/full/nmat2139.html, *Nature Materials*, 2008, **7**, 169.
50. Z. Lv, Y. Fu, S. Hou, D. Wang, H. Wu, C. Zhang, Z. Chu and D. Zou, *Physical Chemistry Chemical Physics*, 2011, **13**, 10076-10083.
51. H. Peng, *Fiber-Shaped Energy Harvesting and Storage Devices*, Springer, 2015.
52. J. Liang, G. Zhang, W. Sun and P. Dong, *Nano Energy*, 2015, **12**, 501-509.
53. Y. P. Fu, M. Peng, Z. B. Lv, X. Cai, S. C. Hou, H. W. Wu, X. Yu, H. Kafafy and D. C. Zou, *Nano Energy*, 2013, **2**, 537-544.
54. G. Liu, M. Peng, W. Song, H. Wang and D. Zou, *Nano Energy*, 2015, **11**, 341-347.
55. J. Liang, G. Zhang, Y. Yang and J. Zhang, *Journal of Materials Chemistry A*, 2014, **2**, 19841-19847.

56. M. Peng, K. Yan, H. Hu, D. Shen, W. Song and D. Zou, *Journal of Materials Chemistry C*, 2015, **3**, 2157-2165.
57. D. Wang, S. C. Hou, H. W. Wu, C. Zhang, Z. Z. Chu and D. C. Zou, *Journal of Materials Chemistry*, 2011, **21**, 6383-6388.
58. Z. Yang, H. Sun, T. Chen, L. Qiu, Y. Luo and H. Peng, *Angewandte Chemie International Edition*, 2013, **52**, 7545-7548.
59. L. Chen, H. Dai, Y. Zhou, Y. Hu, T. Yu, J. Liu and Z. Zou, *Chemical Communications*, 2014, **50**, 14321-14324.
60. X. Cai, S. Hou, H. Wu, Z. Lv, Y. Fu, D. Wang, C. Zhang, H. Kafafy, Z. Chu and D. Zou, *Physical Chemistry Chemical Physics*, 2012, **14**, 125-130.
61. M. J. Uddin, B.Davies, T.J.Dickens and O.I.Okoli, *Solar Energy Materials and Solar Cells*, 2013, **115**, 166-171.
62. F. J. Cai, T. Chen and H. S. Peng, *Journal of Materials Chemistry*, 2012, **22**, 14856-14860.
63. B. Weintraub, Y. G. Wei and Z. L. Wang, *Angewandte Chemie International Edition*, 2009, **48**, 8981-8985.
64. S. Q. Huang, Q. X. Zhang, X. M. Huang, X. Z. Guo, M. H. Deng, D. M. Li, Y. H. Luo, Q. Shen, T. Toyoda and Q. B. Meng, *Nanotechnology*, 2010, **21**, 375201.
65. J. F. Yu, D. Wang, Y. N. Huang, X. Fan, X. Tang, C. Gao, J. L. Li, D. C. Zou and K. Wu, *Nanoscale Research Letters*, 2011, **6**, 94.
66. X. Fan, Z. Z. Chu, L. Chen, C. Zhang, F. Z. Wang, Y. W. Tang, J. L. Sun and D. C. Zou, *Applied Physics Letters*, 2008, **92**, 113510.
67. S. Hao, L. Houpu, Y. Xiao, Y. Zhibin, D. Jue, Q. Longbin and P. Huisheng, *Journal of Materials Chemistry A*, 2014, **2**, 345-349.
68. M. Peng, S. C. Hou, H. W. Wu, Q. Y. Yang, X. Cai, X. Yu, K. Yan, H. W. Hu, F. R. Zhu and D. C. Zou, *Journal of Materials Chemistry A*, 2014, **2**, 926-932.
69. Y. P. Fu, H. W. Wu, S. Y. Ye, X. Cai, X. Yu, S. C. Hou, H. Kafafy and D. C. Zou, *Energy & Environmental Science*, 2013, **6**, 805-812.
70. T. Chen, L. Qiu, Z. Yang, Z. Cai, J. Ren, H. Li, H. Lin, X. Sun and H. Peng, *Angewandte Chemie International Edition*, 2012, **51**, 11977-11980.
71. P. Gao, M. Grätzel and M. K. Nazeeruddin, *Energy & Environmental Science*, 2014, **7**, 2448-2463.
72. S. He, L. Qiu, X. Fang, G. Guan, P. Chen, Z. Zhang and H. Peng, *Journal of Materials Chemistry A*, 2015, **3**, 9406-9410.
73. J. Velten, Z. Kuanyshbekova, Ö. Göktepe, F. Göktepe and A. Zakhidov, *Applied Physics Letters*, 2013, **102**, 203902.
74. W. Guo, C. Xu, G. Zhu, C. Pan, C. Lin and Z. L. Wang, *Nano Energy*, 2012, **1**, 176-182.
75. S. Pan, Z. Yang, H. Li, L. Qiu, H. Sun and H. Peng, *Journal of the American Chemical Society*, 2013, **135**, 10622-10625.
76. H. C. Weerasinghe, F. Z. Huang and Y. B. Cheng, *Nano Energy*, 2013, **2**, 174-189.
77. T. M. Brown, F. De Rossi, F. Di Giacomo, G. Mincuzzi, V. Zardetto, A. Reale and A. Di Carlo, *Journal of Materials Chemistry A*, 2014, **2**, 10788-10817.
78. J. Yan, M. J. Uddin, T. J. Dickens, D. E. Daramola and O. I. Okoli, *Advanced Materials Interfaces*, 2014, **1**, 1400075.
79. J. Ramier, C. J. G. Plummer, Y. Leterrier, J. A. E. Månson, B. Eckert and R. Gaudiana,

Renewable Energy, 2008, **33**, 314-319.
80. Z. Lv, J. Yu, H. Wu, J. Shang, D. Wang, S. Hou, Y. Fu, K. Wu and D. Zou, *Nanoscale*, 2012, **4**, 1248-1253.
81. Z. Y. Liu and M. Misra, *ACS Nano*, 2010, **4**, 2196-2200.
82. Y. P. Fu, Z. B. Lv, H. W. Wu, S. C. Hou, X. Cai, D. Wang and D. C. Zou, *Solar Energy Materials and Solar Cells*, 2012, **102**, 212-219.
83. L. Chu, L. Y. Li, J. Su, F. F. Tu, N. S. Liu and Y. H. Gao, *Scientific Reports*, 2014, **4**, 4420.
84. L. Chu, J. Su, W. Ahmad, N. Liu, L. Li and Y. Gao, *Materials Research Bulletin*, 2015, **66**, 244-248.
85. C. Xu, C. F. Pan, Y. Liu and Z. L. Wang, *Nano Energy*, 2012, **1**, 259-272.
86. S. Hou, X. Cai, H. Wu, X. Yu, M. Peng, K. Yan and D. Zou, *Energy & Environmental Science*, 2013, **6**, 3356.
87. S. Q. Huang, H. C. Sun, X. M. Huang, Q. X. Zhang, D. M. Li, Y. H. Luo and Q. B. Meng, *Nanoscale Research Letters*, 2012, **7**.
88. X. Cai, S. Hou, X. Yu, H. Wu, M. Peng and D. Zou, *Polymer Bulletin (Chinese)*, 2014, **8**, 69-83.
89. X. Yu, Y. P. Fu, X. Cai, H. Kafafy, H. W. Wu, M. Peng, S. C. Hou, Z. B. Lv, S. Y. Ye and D. C. Zou, *Nano Energy*, 2013, **2**, 1242-1248.
90. S. C. Hou, X. Cai, Y. P. Fu, Z. B. Lv, D. Wang, H. W. Wu, C. Zhang, Z. Z. Chu and D. C. Zou, *Journal of Materials Chemistry*, 2011, **21**, 13776-13779.
91. T. Chen, S. T. Wang, Z. B. Yang, Q. Y. Feng, X. M. Sun, L. Li, Z. S. Wang and H. S. Peng, *Angewandte Chemie-International Edition*, 2011, **50**, 1815-1819.
92. S. Zhang, C. Y. Ji, Z. Q. Bian, R. H. Liu, X. Y. Xia, D. Q. Yun, L. H. Zhang, C. H. Huang and A. Y. Cao, *Nano Letters*, 2011, **11**, 3383-3387.
93. S. Pan, Z. Yang, P. Chen, X. Fang, G. Guan, Z. Zhang, J. Deng and H. Peng, *The Journal of Physical Chemistry C*, 2014, **118**, 16419-16425.
94. W. Guo, C. Xu, X. Wang, S. Wang, C. Pan, C. Lin and Z. L. Wang, *Journal of the American Chemical Society*, 2012, **134**, 4437-4441.
95. X. Cai, H. W. Wu, S. C. Hou, M. Peng, X. Yu and D. C. Zou, *Chemsuschem*, 2014, **7**, 474-482.
96. S. Hou, X. Cai, H. Wu, Z. Lv, D. Wang, Y. Fu and D. Zou, *Journal of Power Sources*, 2012, **215**, 164-169.
97. S. Mingxuan and C. Xiaoli, *Journal of Power Sources*, 2013, **223**, 74-78.
98. S. Zhang, C. Ji, Z. Bian, P. Yu, L. Zhang, D. Liu, E. Shi, Y. Shang, H. Peng, Q. Cheng, D. Wang, C. Huang and A. Cao, *ACS Nano*, 2012, **6**, 7191-7198.
99. T. Chen, L. Qiu, H. G. Kia, Z. Yang and H. Peng, *Advanced Materials*, 2012, **24**, 4623-4628.
100. H. Sun, X. You, Z. Yang, J. Deng and H. Peng, *Journal of Materials Chemistry A*, 2013, **1**, 12422-12425.
101. J. Yan, M. J. Uddin, T. J. Dickens and O. I. Okoli, *Solar Energy*, 2013, **96**, 239-252.
102. Y. F. Luo, X. Li, J. X. Zhang, C. R. Liao and X. J. Li, *Journal of Nanomaterials*, 2014, 580256.
103. M. J. Uddin, T. J. Dickens, J. Yan, D. O. Olawale, O. I. Okoli, F. Cesano and Asme, *Proceedings of the Asme Conference on Smart Materials, Adaptive Structures and Intelligent Systems*, 2013, **1**, 879-884.

104. G. Sun, X. Wang and P. Chen, *Materials Today*, 2014, DOI:10.1016/j.mattod.2014.1012.1001.

105. T. Chen, L. B. Qiu, Z. B. Cai, F. Gong, Z. B. Yang, Z. S. Wang and H. S. Peng, *Nano Letters*, 2012, **12**, 2568-2572.

106. M. J. Uddin, T. Dickens, J. Yan, R. Chirayath, D. O. Olawale and O. I. Okoli, *Solar Energy Materials and Solar Cells*, 2013, **108**, 65-69.

107. H. J. Feng, S. H. Tao, X. Y. Zhang, J. Li, Z. H. Liu and X. Fan, *Chemical Communications*, 2014, **50**, 3509-3511.

108. S. C. Hou, Z. B. Lv, H. W. Wu, X. Cai, Z. Z. Chu, Yiliguma and D. C. Zou, *Journal of Materials Chemistry*, 2012, **22**, 6549-6552.

109. M. Toivola, M. Ferenets, P. Lund and A. Harlin, *Thin Solid Films*, 2009, **517**, 2799-2802.

110. A. Gagliardi and A. D. Carlo, *Optical and Quantum Electronics*, 2012, **44**, 141-147.

111. A. Gagliardi, M. A. d. Maur and A. D. Carlo, *IEEE Journal of Quantum Electronics*, 2011, **46**, 1214-1221.

112. A. Gagliardi, M. A. d. Maur, D. Gentilini and A. D. Carlo, *Journal of Computational Electronics*, 2011, **10**, 424-436.

113. X. Fan, F. Wang, Z. Chu, L. Chen, C. Zhang and D. Zou, *Applied Physics Letters*, 2007, **90**, 073501.

114. S. K. Balasingam, M. G. Kang and Y. Jun, *Chemical Communications*, 2013, **49**, 11457-11475.

115. H. Dai, Y. Zhou, L. Chen, B. L. Guo, A. D. Li, J. G. Liu, T. Yu and Z. G. Zou, *Nanoscale*, 2013, **5**, 5102-5108.

116. H. Dai, Y. Zhou, Q. Liu, Z. D. Li, C. X. Bao, T. Yu and Z. G. Zhou, *Nanoscale*, 2012, **4**, 5454-5460.

117. K. Fan, R. J. Li, J. N. Chen, W. Y. Shi and T. Y. Peng, *Science of Advanced Materials*, 2013, **5**, 1596-1626.

118. W. He, J. Qiu, F. Zhuge, X. Li, J. H. Lee, Y. D. Kim, H. K. Kim and Y. H. Hwang, *Nanotechnology*, 2012, **23**, 225602.

119. H. Li, Q. Zhao, H. Dong, Q. Ma, W. Wang, D. Xu and D. Yu, *Nanoscale*, 2014, **6**, 13203-13212.

120. M. J. Yun, S. I. Cha, S. H. Seo and D. Y. Lee, *Scientific Reports*, 2014, **4**, 5322.

121. Z. Tachan, S. Ruhle and A. Zaban, *Solar Energy Materials and Solar Cells*, 2010, **94**, 317-322.

122. S. Q. Huang, X. Z. Guo, X. M. Huang, Q. X. Zhang, H. C. Sun, D. M. Li, Y. H. Luo and Q. B. Meng, *Nanotechnology*, 2011, **22**, 315402.

123. J. Liang, J. Yang, G. Zhang and W. Sun, *Electrochemistry Communications*, 2013, **37**, 80-83.

124. L. Chen, Y. Zhou, H. Dai, Z. D. Li, T. Yu, J. G. Liu and Z. G. Zou, *Journal of Materials Chemistry A*, 2013, **1**, 11790-11794.

125. J. Liang, G. Zhang, J. Yin and Y. Yang, *Journal of Power Sources*, 2014, **272**, 719-729.

126. H. Tao, G. J. Fang, W. J. Ke, W. Zeng and J. Wang, *Journal of Power Sources*, 2014, **245**, 59-65.

127. M. Peng, X. Cai, Y. Fu, X. Yu, S. Liu, B. Deng, K. Hany and D. Zou, *Journal of Power Sources*, 2014, **247**, 249-255.

128. R. Liu, M. Wen, X. Fan, J. Du, Z. Liu and C. Tao, *Colloids and Surfaces A: Physicochemical and Engineering Aspects*, 2013, **428**, 32-38.

129. L. H. Zhang, E. Z. Shi, C. Y. Ji, Z. Li, P. X. Li, Y. Y. Shang, Y. B. Li, J. Q. Wei, K. L. Wang, H. W. Zhu, D. H. Wu and A. Y. Cao, *Nanoscale*, 2012, **4**, 4954-4959.
130. H. N. Chen, L. Q. Zhu, H. C. Liu and W. P. Li, *Nanotechnology*, 2012, **23**, 075402.
131. M. J. Uddin, D. E. Daramola, E. Velasquez, T. J. Dickens, J. Yan, E. Hammel, F. Cesano and O. I. Okoli, *Physica Status Solidi (RRL) - Rapid Research Letters*, 2014, **8**, 898-903.
132. H. Sun, Z. Yang, X. Chen, L. Qiu, X. You, P. Chen and H. Peng, *Angewandte Chemie International Edition*, 2013, **52**, 8276-8280.
133. X. Cai, Z. Lv, H. Wu, S. Hou and D. Zou, *Journal of Materials Chemistry*, 2012, **22**, 9639-9644.
134. L. Chen, Y. Zhou, H. Dai, T. Yu, J. Liu and Z. Zou, *Nano Energy*, 2015, **11**, 697-703.
135. Z. Lv, H. Wu, X. Cai, Y. Fu, D. Wang, Z. Chu and D. Zou, *International Journal of Photoenergy*, 2012, 104597.
136. *Beijing Science Vedio: Flexible Fiber Solar Cells* 2013, http://www.bjscivid.org/html/2013/guonei_0517/15545.html.
137. J. H. Kim, H. S. Jung, Y. S. Chi and T. J. Kang, *Solar Energy*, 2012, **86**, 2606-2612.
138. J. H. Kim, Y. S. Chi and T. J. Kang, *Journal of Power Sources*, 2013, **229**, 84-94.
139. G. Xing, N. Mathews, S. S. Lim, N. Yantara, X. Liu, D. Sabba, M. Grätzel, S. Mhaisalkar and T. C. Sum, *Nature Materials*, 2014, **13**, 476-480.
140. M. J. Uddin, B. Davies, T. J. Dickens and O. I. Okoli, *Solar Energy Materials and Solar Cells*, 2013, **115**, 166-171.
141. H. Li, Z. Yang, L. Qiu, X. Fang, H. Sun, P. Chen, S. Pan and H. Peng, *Journal of Materials Chemistry A*, 2014, **2**, 3841-3846.
142. Y. Liu, M. Li, H. Wang, J. M. Zheng, H. M. Xu, Q. H. Ye and H. Shen, *Journal of Physics D-Applied Physics*, 2010, **43**, 205103.
143. Y. Liu, H. Wang, H. Shen and W. Chen, *Applied Energy*, 2010, **87**, 436-441.
144. Y. Wang, Y. Liu, H. Yang, H. Wang, H. Shen, M. Li and J. Yan, *Current Applied Physics*, 2010, **10**, 119-123.
145. Y. Wang, H. Yang and H. Xu, *Materials Letters*, 2010, **64**, 164-166.
146. Z. Yang, J. Deng, X. Sun, H. Li and H. Peng, *Advanced Materials*, 2014, **26**, 2643-2647.
147. Y. Wang, H. Yang and L. Lu, *Journal of Applied Physics*, 2010, **108**, 064510.
148. J. Usagawa, S. S. Pandey, Y. Ogomi, S. Noguchi, Y. Yamaguchi and S. Hayase, *Progress in Photovoltaics: Research and Applications*, 2013, **21**, 517-524.
149. W. Zeng, M. J. Wang, Y. Li, J. W. Wan, H. H. Huang, H. Tao, D. L. Carroll, X. Z. Zhao, D. C. Zou and G. J. Fang, *Journal of Power Sources*, 2014, **261**, 75-85.
150. G. Kapil, J. Ohara, Y. Ogomi, S. S. Pandey, T. L. Ma and S. Hayase, *RSC Advances*, 2014, **4**, 22959-22963.
151. G. Kapil, S. S. Pandey, Y. Ogomi, T. Ma and S. Hayase, *Organic Electronics*, 2014, **15**, 3399-3405.
152. Y. P. Fu, Z. B. Lv, S. C. Hou, H. W. Wu, D. Wang, C. Zhang and D. C. Zou, *Advanced Energy Materials*, 2012, **2**, 37-41.
153. W. Wang, Q. Zhao, H. Li, H. W. Wu, D. C. Zou and D. P. Yu, *Advanced Functional Materials*, 2012, **22**, 2775-2782.
154. Y. Chae, S. J. Kim, J. H. Kim and E. Kim, *Dyes and Pigments*, 2015, **113**, 378-389.
155. S. W. Pan, Z. B. Yang, P. N. Chen, J. Deng, H. P. Li and H. S. Peng, *Angewandte Chemie*

International Edition, 2014, **53**, 6110-6114.
156. M. Peng, X. Yu, X. Cai, Q. Yang, H. Hu, K. Yan, H. Wang, B. Dong, F. Zhu and D. Zou, *Nano Energy*, 2014, **10**, 117-124.
157. T. Chen, Z. Yang and H. Peng, *Chemphyschem*, 2013, **14**, 1777-1782.
158. H. Sun, X. You, J. Deng, X. Chen, Z. Yang, P. Chen, X. Fang and H. Peng, *Angewandte Chemie International Edition*, 2014, **53**, 6664-6668.
159. X. Chen, H. Sun, Z. Yang, G. Guan, Z. Zhang, L. Qiu and H. Peng, *Journal of Materials Chemistry A*, 2014, **2**, 1897-1902.
160. Z. Zhang, X. Chen, P. Chen, G. Guan, L. Qiu, H. Lin, Z. Yang, W. Bai, Y. Luo and H. Peng, *Advanced Materials*, 2014, **26**, 466-470.
161. Z. Yang, J. Deng, H. Sun, J. Ren, S. Pan and H. Peng, *Advanced Materials*, 2014, **26**, 7038-7042.
162. C. Pan, W. Guo, L. Dong, G. Zhu and Z. L. Wang, *Advanced Materials*, 2012, **24**, 3356-3361.
163. F. C. Krebs and M. Hosel, *Chemsuschem*, 2015, **8**, 966-969.

Flexible Fiber/Wire Shaped Solar Cells in Progress: Properties, Materials, and Designs

Ming Peng[a] and Dechun Zou[a, b, c*]

[*] Prof. Dechun Zou (E-mail: dczou@pku.edu.cn)

[a]Beijing National Laboratory for Molecular Sciences, Key Laboratory of Polymer Chemistry and Physics of Ministry of Education, College of Chemistry and Molecular Engineering, Peking University, Beijing 100871, China. Tel/Fax: +86-10-6275-9799.

[b]Beijing Research Center of Active Matrix Display Technology, Peking University, Beijing 100871, China.

[c]Beijing Institute of Nanoenergy and Nanosystems, Chinese Academy of Science, Beijing 100083, China.

Development of various fiber/wire-shaped solar cells, conventional materials, device properties, innovative designs, and integrated power systems are reviewed.